LLMZERO: Discovering Adaptive Training Strategies for RL Post-Training via LLM Agents

Haoyang Fang[†], **Wei Zhu**[†*], **Boran Han**[†], **Alex Zhang**,
Zhenyu Pan[*], **Shuo Yang**[*], **Shuai Zhang**[*], **Jiading Gai**[*], **Peng Tang**,
Cuixiong Hu[*], **Xuan Zhu**[*], **Huzefa Rangwala**[*], **George Karypis**[*], **Bernie Wang**[†*]
Amazon
{haoyfang, weizhuq, boranhan, yuyawang}@amazon.com

arXiv:2606.18388v2 [cs.LG] 2 Sep 2026

Abstract

RL post-training strategies are dataset-dependent and reveal a recurring empirical pattern: capacity parameters accumulate monotonically across stages, while regularization parameters predominantly oscillate in response to shifting training dynamics. This distinction highlights a potential flaw in fixed training schedules: by forcing all parameters along rigid paths, they fail to capture the dynamic exploration-exploitation tradeoffs that regularization must track. We uncover this through LLMZERO, an agentic system that optimizes training trajectories via tree search by diagnosing pathologies at each checkpoint and proposing coordinated multi-parameter transitions. Across four diverse GRPO tasks, LLMZERO discovers strategies that improve over the base model by 9% to 140% and over grid search by 6% to 15% (relative), consistently outperforming random search and a skill-based agent under a matched compute budget. The capacity–regularization asymmetry is consistent across all four tasks, offering a candidate design heuristic for multi-stage training.

1 Introduction

Fixed training schedules are suboptimal for RL post-training (Lv et al., 2025; Wang et al., 2025a). In most recent works, the community has converged on a narrow set of progressive scheduling techniques with all other hyperparameters held constant, applied identically regardless of dataset, model size, or emergent training dynamics. The dominant approach is gradually increasing response length (Luo et al., 2025b; Chen et al., 2025a; He et al., 2025; Hao et al., 2025; Xiaomi et al., 2025; Luo et al., 2025a; Chen et al., 2025b; Luo et al., 2026; Ji et al., 2025). Others gradually increase rollouts (Luo et al., 2025b; Chen et al., 2025a; Song et al., 2025; Luo et al., 2026), stage training data by progressive difficulty (Chen et al., 2025a; Song et al., 2025; He et al., 2025; Lai and Nissim, 2026; Wan et al., 2025; Luo et al., 2026; Ji et al., 2025), or adopt an oscillating response length schedule (Song et al., 2025). This practice is motivated by training base models to produce increasingly long chains of thought, but is less well-justified for continued training on models that already generate extended reasoning. These guidebook-driven schedules do not systematically specify *when* to trigger a transition, *how much* to adjust, or *which* parameters to change across different tasks. When training dynamics deviate from expectations (KL divergence spikes, model collapse, stagnating validation), no systematic mechanism responds.

To address this, we propose LLMZERO[1], an agent-driven system that searches over training trajectories. The strategies LLMZERO discovers reveal a recurring structural asymmetry: *capacity parameters (response length, rollouts) accumulate monotonically across all four tasks, while regularization parameters (learning rate, KL coefficient, temperature) predominantly oscillate*. Capacity parameters are information-constructive, e.g., shortening response length truncates learned generations and raises gradient variance. Regularization parameters track a non-stationary tradeoff where the optimal exploration-exploitation balance shifts continuously during training, making monotonic decay a poor fit in practice. This pattern manifests differently per task (ChemCoTBench (Li et al., 2026) uses 5-stage progressive stabilization with reactive KL spikes, SSMR-Bench (Wang et al., 2025b) benefits from LR/KL oscillation with monotonic

[†]LLMZero Project Core Team.
[*]Work done at Amazon.

[1]Code will be released at: https://github.com/amazon-science/LLMZero. Until then, please contact haoyfang@amazon.com.

capacity expansion, and PaperSearchQA (Burgess et al., 2026) uses a "tighten then loosen" pattern to escape convergence plateaus), but the underlying asymmetry between parameter classes is consistent across our four evaluated tasks (§4.3).

Traditional adaptive controllers (e.g., proportional KL adjustment (Schulman et al., 2017)) fall short in this setting because they tune only one parameter based on one signal. The strategies we discover require *coordinated* multi-dimensional transitions that change 3+ parameters at once, such as simultaneously raising learning rate to escape a plateau while increasing KL penalty to prevent larger steps from causing divergence. These coordinated interventions require understanding the causal relationships between parameters and training dynamics, which is what LLM reasoning provides (Appendix D.3 gives a full trace).

LLMZERO builds a tree of training trajectories where LLM agents analyze training dynamics through textual metrics and visual plots, and then propose targeted hyperparameter transitions conditioned on the observed training state. An agentic early stopper terminates unpromising branches in real time, reallocating compute toward more promising branches. A modified Monte Carlo Tree Search (MCTS) balances deepening promising branches against exploring alternatives, while checkpoint-based branching enables multi-stage strategies (§3.2).

Across ChemCoTBench, PaperSearchQA, SSMR-Bench, and WildSci (Liu et al., 2026), LLMZERO achieves relative gains of 9–140% over the base model and 6–15% over grid search, and surpasses random search and the skill-based agent under a matched compute budget (§4; Appendix B.3). Notably, LLMZERO finds its best strategy within the first 12 iterations on 3 of 4 tasks, demonstrating its high search efficiency.

Beyond the system itself, our findings demonstrate that optimal strategies are dataset-dependent and not well captured by fixed guidebooks (§4.3.2). Furthermore, LLMZERO consistently improves over base configurations from 0.6B to 8B parameters, indicating that dynamics-aware strategy search generalizes robustly across model scales (§4.4).

2 Preliminary

2.1 Training Strategy Formalization

We formalize three paradigms of increasing complexity for RL post-training. Let M_0 denote the base model, Θ the hyperparameter space, $\mathcal{H}_t = \{(s_1, r_1), \ldots, (s_t, r_t)\}$ the training history up to step t, and μ a validation metric.

Definition 1 (Single-Stage Training)**.** *A single-stage strategy selects one fixed configuration and trains to completion:*

$$\sigma_{\textit{static}} = \langle(\theta, 0)\rangle, \quad \theta^* = \arg\max_{\theta \in \Theta} \mu(\mathcal{T}(M_0, \theta)) . \tag{1}$$

HPO methods (grid, random, Bayesian) search over Θ by running multiple independent static trials.

Definition 2 (Multi-Stage Training)**.** *A multi-stage strategy is a* guidebook-driven *sequence of $L > 1$ phases:*

$$\sigma_{\textit{multi}} = \langle(\theta_1, k_1), (\theta_2, k_2), \ldots, (\theta_L, k_L)\rangle, \quad \theta_\ell \in \Theta,\ k_\ell \in \mathbb{N}, \tag{2}$$

where phase ℓ trains with configuration θ_ℓ starting from step k_ℓ. The schedule structure is specified before training begins and does not systematically depend on training history $\mathcal{H}_t$.

Definition 3 (Adaptive Training)**.** *An adaptive strategy selects both the configuration and the checkpoint to resume from based on observations from prior phases. A transition policy π selects:*

$$(\theta_\ell,\ k_\ell,\ j_\ell) = \pi(\{(\theta_i, k_i, j_i, \mathcal{H}_i)\}_{i<\ell}) , \tag{3}$$

where $j_\ell \in \{1, \ldots, \ell-1\}$ identifies which prior phase to resume from. The policy can backtrack to any earlier checkpoint, enabling branching. Neither the number of phases, configurations, transition points, nor resumption targets are determined before training begins.

RL training is inherently non-stationary: the pace at which exploration must yield to exploitation depends on the dataset, model size, and reward structure, all of which are difficult to predict before training begins. An adaptive strategy can respond in real time, but the space of possible transition policies is vast, motivating automated search.

3 LLMZERO

LLMZERO (Figure 1) builds a tree of training trajectories where each branch point represents a hyperparameter transition chosen based on observed training dynamics. This section describes how the system discovers adaptive strategies.

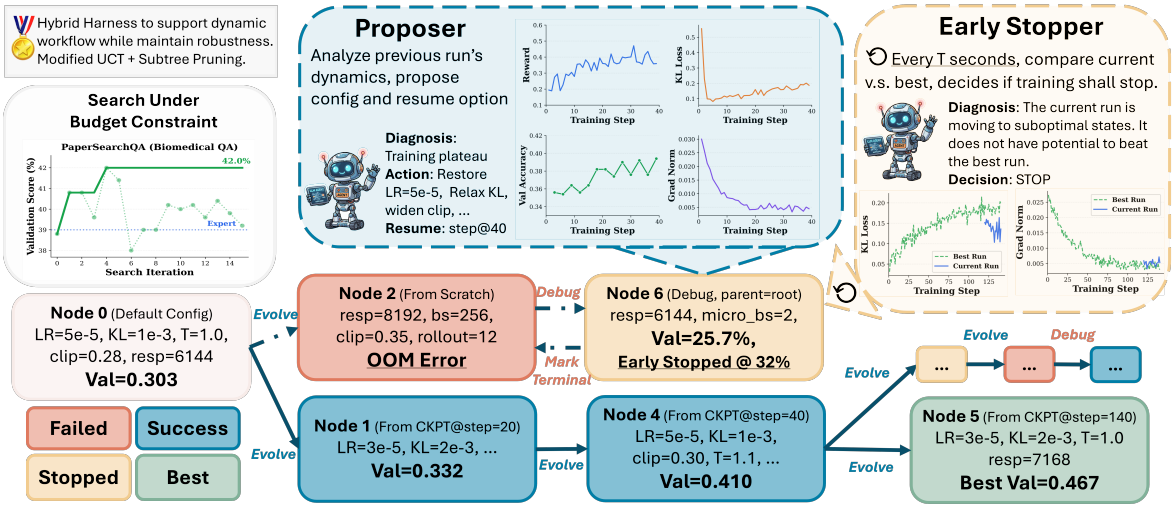

Figure 1: Overview of LLMZERO. The system builds a tree of training trajectories where each node stores a full hyperparameter configuration and resumes from a parent checkpoint, composing multi-stage adaptive strategies via backtracking. At each iteration, the *proposer agent* analyzes training dynamics (rewards, KL divergence, validation scores, gradient norms) through both text summaries and visual plots, then proposes a new configuration with a checkpoint to resume from. During training, the *early stopper* periodically overlays the current run's trajectory against the best completed strategy and terminates dominated runs. Metric values and scores are purely illustrative and do not reflect an actual training run.

3.1 Problem Formulation

Given a dataset $\mathcal{D} = \{(x_i, m_i)\}_{i=1}^{N}$, a base model M_0, a training procedure $\mathcal{T}$, and a validation metric $\mu : \mathcal{Y} \times \mathcal{M} \to [0, 1]$, we seek an adaptive strategy σ^* maximizing held-out performance:

$$\sigma^* = \arg\max_{\sigma} \mathbb{E}_{(x,m)\sim\mathcal{D}_{\text{val}}} \big[\mu\big(\mathcal{T}(M_0, \sigma)(x), m\big)\big], \quad \text{s.t.} \quad \#\text{iterations} \le B, \tag{4}$$

where $\sigma = \langle(\theta_1, k_1), \ldots, (\theta_L, k_L)\rangle$ is constructed online (§2.1) under a small budget B (typically 4–16 iterations, each requiring hours of GPU time).

We model the search as a tree problem. Each node represents one training phase. The root uses a default configuration. Children are created by resuming from a parent checkpoint with modified hyperparameters (*evolving*), by fixing failed runs (*debugging*), or by starting fresh to maintain diversity. Each scratch-to-leaf path forms a candidate multi-stage strategy, and siblings reuse the same parent checkpoint for compute sharing.

3.2 Tree Search and Subtree Pruning

LLMZERO performs a modified MCTS over training trajectories. Each iteration selects a node via UCT, expands it by proposing a hyperparameter transition (or debugging a failure), executes the training phase, and backpropagates the validation score. We adopt a UCT variant (Fang and Wang, 2026) with scale-invariant scoring and virtual child competition; details are reproduced in Appendix F for completeness.

Subtree pruning. A node is marked *terminal* when it can no longer produce children, and terminal subtrees are excluded from selection. When a failed run is fixed, the successful descendant is reparented as a sibling of the oldest ancestor in the debug chain, and the entire subtree below is pruned. Terminality propagates upward: a node becomes terminal when fully expanded with all children terminal.

The search loop. Algorithm 1 (Appendix F) details the complete procedure. The key mechanisms are: (1) a *proposer agent* that performs multimodal analysis of training dynamics (§3.4), (2) an *agentic early stopper* that terminates unpromising runs in real time (§3.5), and (3) forced from-scratch injection to maintain diversity (§3.3).

3.3 Checkpoint-Based Strategy Composition

When an evolve node is created, it loads its parent's model weights at step k and continues training with modified hyperparameters. Successive transitions compose into a multi-stage strategy along the scratch-to-leaf path.

We resume only the **model weights**, reinitializing optimizer state and dataloader position. This

allows arbitrary configuration changes at each transition (batch size, learning rate, optimizer type) while avoiding inheritance of suboptimal momentum accumulators. Because each checkpoint must persist on disk for potential future resumption, storage cost grows linearly with tree depth and training steps. We use LoRA throughout and save only the adapter weights at each checkpoint. This design choice means the LoRA rank is fixed across all phases of a strategy and cannot be modified at transitions.

Forced from-scratch injection. To prevent the search from exclusively exploiting a potentially suboptimal initial configuration, we enforce a minimum from-scratch ratio $\rho_{\min} = 0.2$. When $n_{\text{scratch}}/n_{\text{evolve}} < \rho_{\min}$, we select the best-scoring node n^*, create a from-scratch child that does not count against n^*'s branching limit, and withhold checkpoint information from the proposer to ensure a fresh strategy. This is the primary mechanism by which LLMZERO escapes a poor default configuration. Otherwise, a bad initial run would anchor all subsequent evolve nodes to a weak checkpoint. This mechanism serves as a robustness safeguard rather than a primary driver of performance: on all four tasks the best strategy originates from the root subtree, so the injection mechanism was not triggered in these primary evaluations (Appendix B.3); its value surfaces only under a poor default, where it lifts performance from 51.5% to 56.1% (KL=10^{-2}; Appendix E.3).

3.4 Dynamics-Aware Transition Proposal

The proposer agent is the core adaptive component. It receives the parent node's training configuration, text summaries of step-level metrics, and the best validation score. It also performs *visual reasoning* over per-metric training curve plots, enabling pattern recognition such as trend inflections, divergence onset, and plateau detection that textual summaries alone may miss. Its reasoning proceeds in four stages: (1) *diagnose* the parent run's training health from primary metrics and diagnostic signals; (2) propose *coordinated hyperparameter changes* that address the diagnosed issue, reasoning about causal dependencies between parameters (e.g., raising LR to escape a plateau while increasing KL penalty to prevent divergence); (3) select a *resumption checkpoint* (either a specific step or from scratch); and (4) compute the *epoch budget* based on the chosen batch size and checkpoint step. To mitigate common LLM hallucinations or misinterpretations of domain-specific GRPO/PPO metrics, we inject human-written descriptions to ground the agent's reasoning without restricting which parameters it can modify (Appendix H). The full prompt template is in Appendix I.1.

3.5 Agentic Early Stopping

At 15-minute intervals during training, the early stopper samples current metrics and generates overlay plots comparing the current run's trajectory against the best completed strategy. It outputs `CONTINUE` or `STOP` with explicit reasoning about whether the current trajectory is likely to surpass the incumbent's performance (full prompt in Appendix I.2). Across all 4 tasks, the early stopper terminated 62.1% of nodes before completion, reducing total GPU consumption by an estimated 40–60% relative to running all nodes to completion.

3.6 Automated Pipeline

LLMZERO includes an automated pipeline that handles data preparation, reward function implementation, training code generation, and job execution. In our evaluation, data processing and reward functions are fixed across all methods to ensure a fair comparison. The adaptive strategy search follows a fixed workflow; the essential LLM-based components are the **proposer agent** (§3.4) and the **agentic early stopper** (§3.5). Pipeline details are in Appendix B.

4 Experiments

We evaluate LLMZERO across 4 diverse GRPO tasks to answer: **(RQ1)** Can adaptive strategies outperform static configurations? **(RQ2)** Are discovered patterns dataset-dependent? **(RQ3)** How does performance scale with model size? **(RQ4)** How do individual components contribute? **(RQ5)** Do strategies transfer across tasks?

4.1 Setup

Tasks. We evaluate on ChemCoTBench (Li et al., 2026), PaperSearchQA (Burgess et al., 2026), SSMR-Bench (Wang et al., 2025b), and WildSci (Liu et al., 2026). Each dataset is uniformly subsampled to 5,000 train, 500 validation, and 500 test examples to keep per-iteration training time tractable for search. All tasks use GRPO via VeRL (Sheng et al., 2024) (Appendix B.1).

Table 1: Main results: test score (%) at the best validation node within 16 iterations on Qwen3-4B. **Bold**: best per column (aggregate only). Underline: second best. Subscripts show gain over the base model. ChemCoT reports category-averaged test accuracy across 3 task families (mol. optimization, 6 subtasks at 0% for all methods, is omitted). SSMR shows per-subtask test scores (Scl=scale, Bea=beat, Cho=chord, Int=interval). WildSci practitioner config scores below Qwen3-4B on weighted test aggregate due to domain-level trade-offs (see §4.3.1).

		ChemCoT (Chem)				**PaperSearchQA**	**SSMR** (Music)					**WildSci**
	Type	Und	Edit	Rxn	Avg	Bio	Scl	Bea	Cho	Int	Avg	Sci
Qwen3-4B	–	40.5	8.0	2.3	16.9	31.6	60.0	44.8	50.4	50.4	51.4	53.6
Practitioner	Static	$61.1_{(+20.6)}$	$23.0_{(+15.0)}$	$14.9_{(+12.6)}$	$33.0_{(+16.1)}$	$39.0_{(+7.4)}$	$76.8_{(+16.8)}$	$60.0_{(+15.2)}$	$65.6_{(+15.2)}$	$60.8_{(+10.4)}$	$65.8_{(+14.4)}$	$53.2_{(-0.4)}$
Random search	Static	$66.4_{(+25.9)}$	$23.0_{(+15.0)}$	$28.7_{(+26.4)}$	$\underline{39.4}_{(+22.5)}$	$37.6_{(+6.0)}$	$90.4_{(+30.4)}$	$77.6_{(+32.8)}$	$68.8_{(+18.4)}$	$60.8_{(+10.4)}$	$74.4_{(+23.0)}$	$55.8_{(+2.2)}$
Grid search	Static	$61.2_{(+20.7)}$	$23.4_{(+15.4)}$	$20.9_{(+18.6)}$	$35.2_{(+18.3)}$	$39.0_{(+7.4)}$	$87.2_{(+27.2)}$	$84.0_{(+39.2)}$	$69.6_{(+19.2)}$	$69.6_{(+19.2)}$	$77.6_{(+26.2)}$	$53.0_{(-0.6)}$
Skill-based LLM agent	Adaptive	$61.8_{(+21.3)}$	$21.4_{(+13.4)}$	$27.7_{(+25.4)}$	$37.0_{(+20.1)}$	$\underline{40.2}_{(+8.6)}$	$96.0_{(+36.0)}$	$88.0_{(+43.2)}$	$74.4_{(+24.0)}$	$61.6_{(+11.2)}$	$\underline{80.0}_{(+28.6)}$	$\underline{56.6}_{(+3.0)}$
LLMZero	**Adaptive**	$69.8_{(+29.3)}$	$33.3_{(+25.3)}$	$18.5_{(+16.2)}$	$\mathbf{40.5}_{(+23.6)}$	$\mathbf{42.6}_{(+11.0)}$	$94.4_{(+34.4)}$	$81.6_{(+36.8)}$	$77.6_{(+27.2)}$	$75.2_{(+24.8)}$	$\mathbf{82.2}_{(+30.8)}$	$\mathbf{58.5}_{(+4.9)}$

Models. Primary evaluation uses **Qwen3-4B** (LoRA, rank=64). Scaling analysis spans **Qwen3-0.6B** through **8B**. Base model evaluation: greedy decoding, max response length=8192. Infrastructure: Ray clusters on EKS, 32–64 A100 40G GPUs.

Baselines. We compare against: (1) a **practitioner baseline** (fixed GRPO recipe tuned on separate tasks), (2) **random search** (8 trials from broad HP ranges), (3) **grid search** (8 trials over LR × LoRA rank, selected as the most efficient range based on internal experience), and (4) a **skill-based LLM agent** built on Claude Code as the orchestration backend with Claude Opus 4.6 at high reasoning effort, which autonomously plans iterations and can stop/resume from any checkpoint without tree search or visual reasoning. Because its autonomous orchestration maintains full conversation context, it costs 73× more in API overall than LLMZero with its fixed workflow, limiting it to 6–9 iterations in practice. Full baseline configurations are in Appendix B; budget fairness details are in Appendix B.3.

4.2 Main Results (RQ1)

Table 1 presents the test score at the best validation step for each method. The comparison isolates two questions. First, does adaptive beat static (LLMZero vs. practitioner/random/grid search)? Second, does the fixed workflow with tree search outperform a general-purpose LLM agent (LLMZero vs. skill-based LLM agent)? LLMZero outperforms all static baselines on every task. Notably, the WildSci practitioner config scores below the base model (53.2% vs. 53.6%), yet LLMZero recovers to 58.5%. Capping LLMZero at a matched 8 iterations (within the skill agent's 6–9 range), it still matches or exceeds the skill agent on all four tasks (Appendix D.1). Appendix D collects further analysis

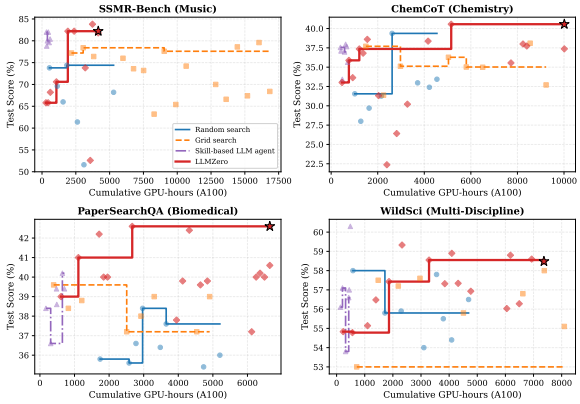

Figure 2: Test score at the best-validation run so far vs. cumulative GPU-hours. Dots show per-run/node test scores; step curves track the test score of whichever run has the highest validation so far.

of these results, including the detailed 8B OOM recovery, a full proposer reasoning trace, and failure modes beyond compute limits.

Compute efficiency. Figure 2 plots best-so-far test score against cumulative GPU-hours for each method. LLMZero reaches the highest final test score on all 4 tasks under comparable total GPU compute (4,159–10,013 GPU-hours for LLMZero vs. 4,543–16,846 for HPO baselines). Early stopping terminates 56–70% of nodes before completion. The forced from-scratch injection (§3.3) explains why LLMZero uses more total training time than the skill-based agent.

API cost. LLMZero's fixed workflow consumes 73× less API cost overall (44–144× per task) than the skill-based agent ($48 vs. $3,545 total; Table 5 in Appendix B.4).

4.3 Analysis of Discovered Strategies (RQ2)

We examine whether the adaptive strategies LLMZero discovers are dataset-dependent and

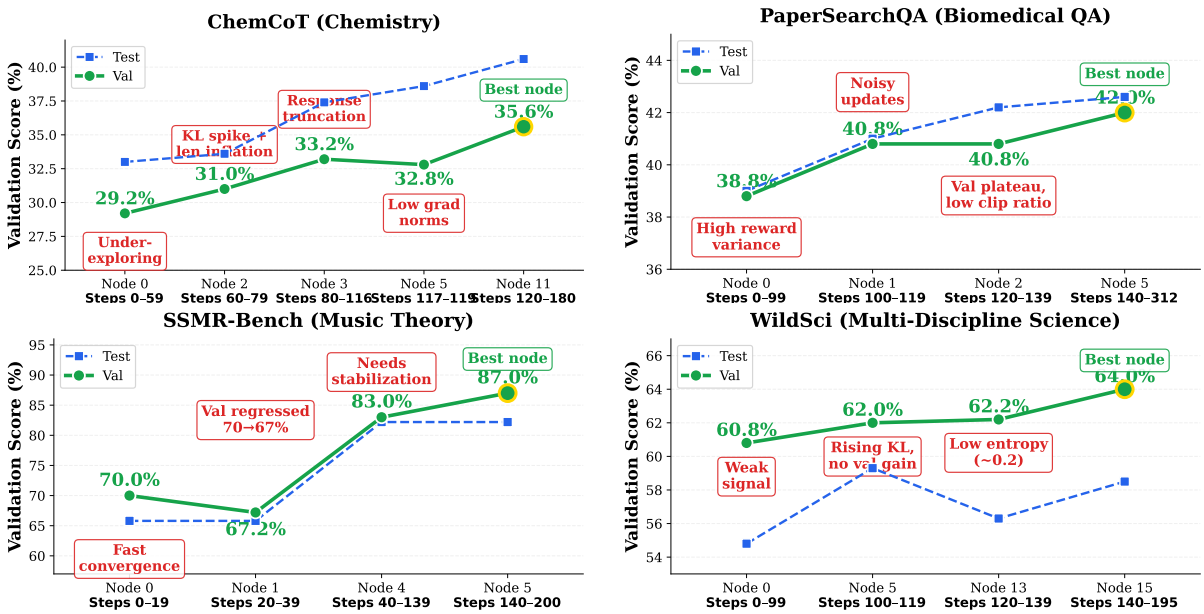

Figure 3: Best adaptive strategies across all four tasks. Green solid: validation score. Blue dashed: test score. Each point is one phase with annotations summarizing observed training dynamics.

what structural patterns emerge. Figure 3 visualizes the best strategy for each task. We analyze ChemCoT and SSMR-Bench below; the PaperSearchQA and WildSci strategies are described in Appendix C.4.

4.3.1 Per-Dataset Strategies

ChemCoT (Chemistry). The best strategy is a 5-phase chain (Figure 3). After initial training (val=29.2%), the system widens the clip range and enables advantage normalization while lowering temperature (Phase 2, val=31.0%), then observes a 16× KL loss spike coinciding with response length inflation (1630→2278 tokens) without validation improvement, responding with a 5× KL penalty increase (Phase 3, val=33.2%). This KL divergence spike preceded validation degradation by 1–2 phases, suggesting KL as a leading indicator that practitioners should monitor proactively. Phase 4 expands response capacity (6144→7168 tokens) with a transient regression (val=32.8%), before Phase 5 addresses low gradient norms (<0.001) and flat validation by raising LR and rollouts while reducing batch size (val=35.6%).

Failure case: molecular optimization. Nine subtasks (all `mol_opt_*`, `rxn_retro`, `rxn_nepp`, `rxn_mechanism`) score 0% across all methods including LLMZERO. Molecular optimization requires valid SMILES string generation, which is a learned structural capability rather than a reasoning capability. No training strategy can elicit a skill the base model fundamentally lacks at 4B scale. This demonstrates the boundary of adaptive scheduling: it optimizes *how* to train but cannot compensate for missing model capacity. See Appendix D.4 for more details and further failure analysis.

SSMR-Bench (Music Theory). The best strategy is a 4-phase chain (Figure 3). From Phase 1 (val=70.0%), Phase 2 applies multiple conservative changes simultaneously: reducing LR to 3e-5, doubling KL to 0.002, reducing gradient clipping to 0.5, enabling advantage normalization, and raising temperature to 1.1. This over-constrains learning and causes regression to 67.2%. Phase 3 reverses the core constraints (restoring LR to 5e-5, relaxing KL to 0.001, widening clip to 0.30) while retaining the higher temperature, driving a +15.8 pp recovery (val=83.0%). Phase 4 re-tightens for convergence (LR=3e-5, KL=0.002, T=1.0) with expanded response length (6144→7168 tokens), reaching val=87.0% (test=82.2%). LR and KL oscillate across phases while epochs and response capacity accumulate monotonically. The agentic early stopper terminated 7 of 10 explored nodes.

4.3.2 Cross-Task Structural Patterns

Three empirical observations emerge from comparing strategies across tasks:

Dataset-specific dynamics determine strategy structure. Each task shows a distinct observable pattern: KL divergence spikes with response-length inflation (ChemCoT), stagnating validation with near-zero clip ratios (PaperSearchQA), validation regression under conservative hyperparameters (SSMR-Bench), and model collapse after aggressive LR scaling (WildSci). These emerge unpredictably (ChemCoT's KL spike appears only after 2 phases) and require severity-calibrated interventions, which the KL trajectories mirror: reactive spikes, monotonic increase, symmetric oscillation, and tighten-then-relax, respectively. No fixed schedule can anticipate which pattern will dominate or when.

Multi-dimensional transitions are effective. In all 4 tasks, the highest-gain transition changes 3+ hyperparameters in coordinated combinations; e.g., ChemCoT Phase 5 jointly raises LR and KL penalty, which the proposer reasoned would escape the plateau without diverging. Such interventions are unlikely to be found by tuning parameters independently.

Notably, the KL coefficient is the most frequently adjusted parameter (changed in 12 of 13 transitions), yet it is held constant in all surveyed multi-stage works (§1). Its non-monotonic trajectory appears load-bearing: the best strategies tighten KL reactively and relax it proactively, so a fixed KL schedule would miss these dynamics on most tasks.

Capacity parameters accumulate while regularization parameters oscillate. Across all 4 best strategies, response length and rollout count show *zero* direction reversals, while LR and temperature reverse 1–2 times on every task; the KL coefficient reverses on 3 of 4 tasks but rises monotonically on PaperSearchQA, where it progressively tightens to stabilize noisy updates. We read this as a candidate design heuristic: *capacity parameters should accumulate monotonically while regularization parameters should be free to oscillate in response to shifting training dynamics.* The asymmetry may reflect that capacity parameters are information-constructive (reducing them truncates reasoning chains or raises gradient variance), while regularization parameters control an exploration-exploitation tradeoff whose optimal balance shifts continuously. The pattern is not an artifact of directional prompt cues: of all metric-tracked hyperparameters (Appendix H.2), only the KL coefficient and the maximum response length carry a single directional hint, yet behavior splits by parameter class, not hint direction. KL oscillates despite a hint suggesting only conditional increase, and monotonic response-length accumulation is independently corroborated by prior multi-stage RL work (Luo et al., 2025b; Chen et al., 2025a; Luo et al., 2025a; Xiaomi et al., 2025). An off-best-path ChemCoT node did reduce capacity parameters (rollouts 8→4), so the search space is not one-directional. We nonetheless scope the heuristic to our evaluated setting; its generality across architectures, optimizers, reward structures, dataset sizes, and RL algorithms remains to be established.

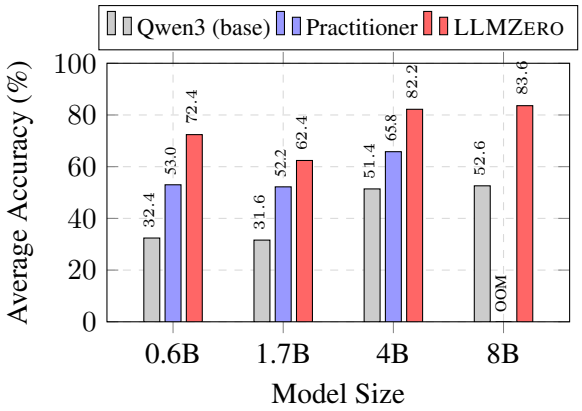

Figure 4: Model scaling on SSMR-Bench (average across 4 subtasks). Practitioner config failed (OOM) on 8B. Per-subtask breakdown in Table 7 (Appendix C.3).

Diagnosis quality. We human-verified every observation in the proposer's diagnoses against metric traces (Tables 8–11); all are correct. Of 13 non-initial transitions, 11 improve validation. On 3 of 4 tasks test scores increase monotonically along the best path (Figure 3); on WildSci one transition regresses but the next recovers.

4.4 Scaling Analysis (RQ3)

Figure 4 reports average accuracy on SSMR-Bench across model sizes. LLMZero consistently outperforms baselines from 0.6B to 8B, with gains of +30.8 pp to +40.0 pp over the base model. The practitioner config failed with OOM on 8B, while LLMZero autonomously discovered a working configuration (83.6%). Note that OOM recovery is not a fundamental capability of the method, since a practitioner could resolve it manually by adjusting memory settings. LLMZero navigated the failure autonomously as a proof of its robustness. A detailed breakdown of the diagnosis and the decisive

configuration changes is in Appendix D.2.

4.5 Ablation Studies (RQ4)

Table 2 ablates key components on SSMR-Bench to distinguish which drive accuracy gains versus compute efficiency. Removing multi-stage composition drops accuracy by 9.4 pp (82.2%→72.8%), confirming that the ability to compose adaptive multi-stage strategies is the primary driver of improvement; without it, the system reduces to selecting the best single-phase configuration from the same search budget. Removing visual reasoning or early stopping yields on-par accuracy, but at substantially worse compute efficiency. Visual reasoning enables the early stopper to reliably judge trajectory dominance from overlay plots, while early stopping itself focuses compute on promising branches. Together they reduce wall-clock time without sacrificing strategy quality. The small accuracy gaps from removing visual reasoning or early stopping sit within single-seed variance, and both ablations leave the LLM's text-based reading of dynamics active, so neither isolates the reasoning itself. A reward-only ablation that strips all diagnostic signals does: it drops the test mean from 61.5% to 49.5% on the public VeRL 0.7.1 stack (Appendix E.1); removing the proposer entirely would collapse LLMZERO into the random/grid baselines it already outperforms. See Appendix E for further ablation studies on the public VeRL 0.7.1 stack, including backbone-quality and poor-default from-scratch analyses.

4.6 Strategy Transfer (RQ5)

We test whether multi-stage structure alone drives improvement by executing two fixed schedules on three held-out tasks (Table 3): the discovered SSMR-Bench 4-phase strategy, and a Capacity Guidebook that progressively increases only response length and rollout count following the community practice (Luo et al., 2025b; Chen et al., 2025a) (Table 16), with stage durations estimated from our successful trajectories. Both fixed schedules improve over the base model on all tasks (+4.6 to +24.4 pp for SSMR transfer, +4.8 to +19.7 pp for the Guidebook), confirming that multi-stage training is broadly beneficial. However, their gains are inconsistent: the SSMR transfer nearly matches adaptive search on WildSci (58.3% vs. 58.5%) but underperforms by 6.4 pp on PaperSearchQA, while the Guidebook lags the SSMR transfer by 4.7 pp on ChemCoT. These inconsistencies suggest that fixed schedules do not always reliably generalize across tasks without adapting to observed training dynamics. Notably, the strong transfer performance on some tasks may benefit from identical base model and dataset sizes, which produce similar training dynamics; adaptive search remains necessary for robustness when dataset scale or model family varies (More analysis in Appendix C.6).

Table 2: Ablation on SSMR-Bench: test accuracy (%) at best validation node. Speed is relative compute efficiency normalized to the full system.

Variant	Scl	Bea	Cho	Int	Avg	Speed
LLMZERO (full)	94.4	81.6	77.6	75.2	**82.2**	**1.0**×
w/o visual reasoning	93.6	85.6	80.0	70.4	82.4	0.6×
w/o multi-stage	88.8	78.4	62.4	61.6	72.8	0.22×
w/o early stopping	93.6	90.4	75.2	72.0	82.8	0.29×

Table 3: Strategy transfer: test scores (%) for fixed multi-stage schedules on held-out tasks. SSMR transfer applies the discovered 4-phase strategy. Capacity Guidebook applies only progressive capacity scaling.

Dataset	**Practitioner**	**Random**	**SSMR transfer**	**Cap. Guidebook**	**LLMZERO**
PaperSearchQA	39.0	37.6	36.2	37.8	**42.6**
WildSci	53.2	55.8	**58.3**	**58.4**	**58.5**
ChemCoT	33.0	39.4	**41.3**	36.6	40.5
Average	41.7	44.3	45.3	44.3	**47.2**

5 Conclusion

We observe a recurring structural asymmetry in multi-stage GRPO strategies: capacity parameters (e.g., response length, rollouts) accumulate monotonically, while regularization parameters (e.g., learning rate, KL coefficient, temperature) predominantly oscillate in response to shifting training dynamics. We uncover this through LLMZERO, an agentic system that reasons about training dynamics at each checkpoint and proposes coordinated, multi-parameter transitions to address diagnosed pathologies. Across four diverse tasks, these adaptive strategies improve over the base model by 9% to 140% and over grid search by 6% to 15% (relative), outperforming all baselines. These findings suggest that the current paradigm's narrow focus on staging one or two capacity parameters may constrain models' potential, and that dynamics-aware, multi-dimensional adaptation is beneficial in RL post-training. We leave the extension of this approach beyond GRPO, including to other RL finetuning algorithms, supervised finetuning, and foundation model pretraining, to future work.

Limitations

Our system expands one node at a time; a hybrid with population-based training (Jaderberg et al., 2017) that maintains multiple trajectories with LLM-guided transitions would combine broad exploration with intelligent proposals and is a natural next step. All datasets are subsampled to 5,000 training examples to keep per-iteration search tractable; validating that discovered strategies and structural patterns hold at production data scales and model scales requires substantially more compute and is left to future work.

References

James Bergstra and Yoshua Bengio. 2012. Random search for hyper-parameter optimization. *Journal of Machine Learning Research*, 13(10):281–305.

James Burgess, Jan N. Hansen, Duo Peng, Yuhui Zhang, Alejandro Lozano, Min Woo Sun, Emma Lundberg, and Serena Yeung-Levy. 2026. Papersearchqa: Learning to search and reason over scientific papers with rlvr. *Preprint*, arXiv:2601.18207.

Yang Chen, Zhuolin Yang, Zihan Liu, Chankyu Lee, Peng Xu, Mohammad Shoeybi, Bryan Catanzaro, and Wei Ping. 2025a. Acereason-nemotron: Advancing math and code reasoning through reinforcement learning. *Preprint*, arXiv:2505.16400.

Zhipeng Chen, Yingqian Min, Beichen Zhang, Jie Chen, Jinhao Jiang, Daixuan Cheng, Wayne Xin Zhao, Zheng Liu, Xu Miao, Yang Lu, Lei Fang, Zhongyuan Wang, and Ji-Rong Wen. 2025b. An empirical study on eliciting and improving r1-like reasoning models. *Preprint*, arXiv:2503.04548.

Yizhou Chi, Yizhang Lin, Sirui Hong, Duyi Pan, Yaying Fei, Guanghao Mei, Bangbang Liu, Tianqi Pang, Jacky Kwok, Ceyao Zhang, Bang Liu, and Chenglin Wu. 2024. Sela: Tree-search enhanced llm agents for automated machine learning. *Preprint*, arXiv:2410.17238.

Yaxin Du, Xiyuan Yang, Zhifan Zhou, Wanxu Liu, Zixing Lei, Zimeng Chen, Fenyi Liu, Haotian Wu, Yuzhu Cai, Zexi Liu, and 1 others. 2026. Datamaster: Towards autonomous data engineering for machine learning. *arXiv preprint arXiv:2605.10906*.

Haoyang Fang, Boran Han, Nick Erickson, Xiyuan Zhang, Su Zhou, Anirudh Dagar, Jiani Zhang, Ali Caner Turkmen, Cuixiong Hu, Huzefa Rangwala, Ying Nian Wu, Bernie Wang, and George Karypis. 2025. Mlzero: A multi-agent system for end-to-end machine learning automation. *Preprint*, arXiv:2505.13941.

Haoyang Fang and Bernie Wang. 2026. Exploit more, explore smarter for budget-constrained agentic search. *Preprint*, arXiv:2608.23848.

Daya Guo, Dejian Yang, Haowei Zhang, Junxiao Song, Peiyi Wang, Qihao Zhu, Runxin Xu, Ruoyu Zhang, Shirong Ma, Xiao Bi, Xiaokang Zhang, Xingkai Yu, Yu Wu, Z. F. Wu, Zhibin Gou, Zhihong Shao, Zhuoshu Li, Ziyi Gao, Aixin Liu, and 175 others. 2025. Deepseek-r1 incentivizes reasoning in llms through reinforcement learning. *Nature*, 645(8081):633–638.

Shibo Hao, Yi Gu, Haodi Ma, Joshua Jiahua Hong, Zhen Wang, Daisy Zhe Wang, and Zhiting Hu. 2023. Reasoning with language model is planning with world model. *Preprint*, arXiv:2305.14992.

Yifan Hao, Fangning Chao, Yaqian Hao, Zhaojun Cui, Huan Bai, Haiyu Zhang, Yankai Liu, Chao Deng, and Junlan Feng. 2025. Jt-math: A multi-stage framework for advanced mathematical reasoning in large language models. *Preprint*, arXiv:2507.19748.

Jujie He, Jiacai Liu, Chris Yuhao Liu, Rui Yan, Chaojie Wang, Peng Cheng, Xiaoyu Zhang, Fuxiang Zhang, Jiacheng Xu, Wei Shen, Siyuan Li, Liang Zeng, Tianwen Wei, Cheng Cheng, Bo An, Yang Liu, and Yahui Zhou. 2025. Skywork open reasoner 1 technical report. *Preprint*, arXiv:2505.22312.

Max Jaderberg, Valentin Dalibard, Simon Osindero, Wojciech M. Czarnecki, Jeff Donahue, Ali Razavi, Oriol Vinyals, Tim Green, Iain Dunning, Karen Simonyan, Chrisantha Fernando, and Koray Kavukcuoglu. 2017. Population based training of neural networks. *Preprint*, arXiv:1711.09846.

Yunjie Ji, Sitong Zhao, Xiaoyu Tian, Haotian Wang, Shuaiting Chen, Yiping Peng, Han Zhao, and Xiangang Li. 2025. How difficulty-aware staged reinforcement learning enhances llms' reasoning capabilities: A preliminary experimental study. *Preprint*, arXiv:2504.00829.

Zhengyao Jiang, Dominik Schmidt, Dhruv Srikanth, Dixing Xu, Ian Kaplan, Deniss Jacenko, and Yuxiang Wu. 2025. Aide: Ai-driven exploration in the space of code. *Preprint*, arXiv:2502.13138.

Feiyang Kang, Hanze Li, Adam Nguyen, Mahavir Dabas, Jiaqi W Ma, Frederic Sala, Dawn Song, and Ruoxi Jia. 2026. Can generalist agents automate data curation? *arXiv preprint arXiv:2606.04261*.

Huiyuan Lai and Malvina Nissim. 2026. Tacler: Tailored curriculum reinforcement learning for efficient reasoning. *Preprint*, arXiv:2601.21711.

Hao Li, He Cao, Bin Feng, Yanjun Shao, Xiangru Tang, Zhiyuan Yan, Li Yuan, Yonghong Tian, and Yu Li. 2026. Beyond chemical qa: Evaluating llm's chemical reasoning with modular chemical operations. *Preprint*, arXiv:2505.21318.

Liam Li, Kevin Jamieson, Afshin Rostamizadeh, Ekaterina Gonina, Jonathan Ben-Tzur, Moritz Hardt, Benjamin Recht, and Ameet Talwalkar. 2020. A system for massively parallel hyperparameter tuning. *Proceedings of machine learning and systems*, 2:230–246.

Lisha Li, Kevin Jamieson, Giulia DeSalvo, Afshin Rostamizadeh, and Ameet Talwalkar. 2018. Hyperband: A novel bandit-based approach to hyperparameter optimization. *Preprint*, arXiv:1603.06560.

Tengxiao Liu, Deepak Nathani, Zekun Li, Kevin Yang, and William Yang Wang. 2026. Wildsci: Advancing scientific reasoning from in-the-wild literature. *Preprint*, arXiv:2601.05567.

Michael Luo, Sijun Tan, Roy Huang, Ameen Patel, Alpay Ariyak, Qingyang Wu, Xiaoxiang Shi, Rachel Xin, Colin Cai, Maurice Weber, Ce Zhang, Li Erran Li, Raluca Ada Popa, and Ion Stoica. 2025a. Deepcoder: A fully open-source 14b coder at o3-mini level. Notion Blog.

Michael Luo, Sijun Tan, Justin Wong, Xiaoxiang Shi, William Y. Tang, Manan Roongta, Colin Cai, Jeffrey Luo, Li Erran Li, Raluca Ada Popa, and Ion Stoica. 2025b. Deepscaler: Surpassing o1-preview with a 1.5b model by scaling rl. Notion Blog.

Yun Luo, Futing Wang, Qianjia Cheng, Fangchen Yu, Haodi Lei, Jianhao Yan, Chenxi Li, Jiacheng Chen, Yufeng Zhao, Haiyuan Wan, Yuchen Zhang, Shenghe Zheng, Junchi Yao, Qingyang Zhang, Haonan He, Wenxuan Zeng, Li Sheng, Chengxing Xie, Yuxin Zuo, and 12 others. 2026. P1-vl: Bridging visual perception and scientific reasoning in physics olympiads. *Preprint*, arXiv:2602.09443.

Xingtai Lv, Yuxin Zuo, Youbang Sun, Hongyi Liu, Yuntian Wei, Zhekai Chen, Xuekai Zhu, Kaiyan Zhang, Bingning Wang, Ning Ding, and 1 others. 2025. Towards a unified view of large language model post-training. *arXiv preprint arXiv:2509.04419*.

Alexander Novikov, Ngân Vũ, Marvin Eisenberger, Emilien Dupont, Po-Sen Huang, Adam Zsolt Wagner, Sergey Shirobokov, Borislav Kozlovskii, Francisco J. R. Ruiz, Abbas Mehrabian, M. Pawan Kumar, Abigail See, Swarat Chaudhuri, George Holland, Alex Davies, Sebastian Nowozin, Pushmeet Kohli, and Matej Balog. 2025. Alphaevolve: A coding agent for scientific and algorithmic discovery. *Preprint*, arXiv:2506.13131.

Rafael Rafailov, Archit Sharma, Eric Mitchell, Stefano Ermon, Christopher D. Manning, and Chelsea Finn. 2024. Direct preference optimization: Your language model is secretly a reward model. *Preprint*, arXiv:2305.18290.

Ben Rank, Hardik Bhatnagar, Ameya Prabhu, Shira Eisenberg, Karina Nguyen, Matthias Bethge, and Maksym Andriushchenko. 2026. Posttrainbench: Can llm agents automate llm post-training? *arXiv preprint arXiv:2603.08640*.

John Schulman, Filip Wolski, Prafulla Dhariwal, Alec Radford, and Oleg Klimov. 2017. Proximal policy optimization algorithms. *arXiv preprint arXiv:1707.06347*.

Zhihong Shao, Peiyi Wang, Qihao Zhu, Runxin Xu, Junxiao Song, Xiao Bi, Haowei Zhang, Mingchuan Zhang, Y. K. Li, Y. Wu, and Daya Guo. 2024. Deepseekmath: Pushing the limits of mathematical reasoning in open language models. *Preprint*, arXiv:2402.03300.

Guangming Sheng, Chi Zhang, Zilingfeng Ye, Xibin Wu, Wang Zhang, Ru Zhang, Yanghua Peng, Haibin Lin, and Chuan Wu. 2024. Hybridflow: A flexible and efficient rlhf framework. *arXiv preprint arXiv: 2409.19256*.

Jasper Snoek, Hugo Larochelle, and Ryan P. Adams. 2012. Practical bayesian optimization of machine learning algorithms. *Preprint*, arXiv:1206.2944.

Mingyang Song, Mao Zheng, Zheng Li, Wenjie Yang, Xuan Luo, Yue Pan, and Feng Zhang. 2025. Fastcurl: Curriculum reinforcement learning with stage-wise context scaling for efficient training r1-like reasoning models. *Preprint*, arXiv:2503.17287.

Fanqi Wan, Weizhou Shen, Shengyi Liao, Yingcheng Shi, Chenliang Li, Ziyi Yang, Ji Zhang, Fei Huang, Jingren Zhou, and Ming Yan. 2025. Qwenlong-l1: Towards long-context large reasoning models with reinforcement learning. *Preprint*, arXiv:2505.17667.

Zhenting Wang, Guofeng Cui, Yu-Jhe Li, Kun Wan, and Wentian Zhao. 2025a. Dump: Automated distribution-level curriculum learning for rl-based llm post-training. *arXiv preprint arXiv:2504.09710*.

Zhilin Wang, Zhe Yang, Yun Luo, Yafu Li, Xiaoye Qu, Ziqian Qiao, Haoran Zhang, Runzhe Zhan, Derek F. Wong, Jizhe Zhou, and Yu Cheng. 2025b. Towards an ai musician: Synthesizing sheet music problems for musical reasoning. *Preprint*, arXiv:2509.04059.

Haoming Wen, Yushi Bai, Juanzi Li, and Jie Tang. 2025. Siri: Scaling iterative reinforcement learning with interleaved compression. *Preprint*, arXiv:2509.25176.

LLM-Core Xiaomi, :, Bingquan Xia, Bowen Shen, Cici, Dawei Zhu, Di Zhang, Gang Wang, Hailin Zhang, Huaqiu Liu, Jiebao Xiao, Jinhao Dong, Liang Zhao, Peidian Li, Peng Wang, Shihua Yu, Shimao Chen, Weikun Wang, Wenhan Ma, and 46 others. 2025. Mimo: Unlocking the reasoning potential of language model – from pretraining to posttraining. *Preprint*, arXiv:2505.07608.

Shunyu Yao, Dian Yu, Jeffrey Zhao, Izhak Shafran, Thomas L. Griffiths, Yuan Cao, and Karthik Narasimhan. 2023. Tree of thoughts: Deliberate problem solving with large language models. *Preprint*, arXiv:2305.10601.

Chujie Zheng, Shixuan Liu, Mingze Li, Xiong-Hui Chen, Bowen Yu, Chang Gao, Kai Dang, Yuqiong Liu, Rui Men, An Yang, and 1 others. 2025. Group sequence policy optimization. *arXiv preprint arXiv:2507.18071*.

Contents

1 Introduction **1**

2 Preliminary **2**
- 2.1 Training Strategy Formalization . 2

3 LLMZero **2**
- 3.1 Problem Formulation 3
- 3.2 Tree Search and Subtree Pruning . 3
- 3.3 Checkpoint-Based Strategy Composition 3
- 3.4 Dynamics-Aware Transition Proposal 4
- 3.5 Agentic Early Stopping 4
- 3.6 Automated Pipeline 4

4 Experiments **4**
- 4.1 Setup 4
- 4.2 Main Results (RQ1) 5
- 4.3 Analysis of Discovered Strategies (RQ2) 5
  - 4.3.1 Per-Dataset Strategies . . 6
  - 4.3.2 Cross-Task Structural Patterns 6
- 4.4 Scaling Analysis (RQ3) 7
- 4.5 Ablation Studies (RQ4) 8
- 4.6 Strategy Transfer (RQ5) 8

5 Conclusion **8**

A Related Work **12**

B Experimental Setup Details **13**
- B.1 Task Details 13
- B.2 Baseline Configurations 13
- B.3 Compute Budget Fairness 13
- B.4 API Cost 13
- B.5 Model and Infrastructure 13
- B.6 LLMZero Configuration 14
- B.7 Skill-Based LLM Agent 14

C Additional Results and Analysis **15**
- C.1 Search Convergence 15
- C.2 ChemCoT Per-Subtask Breakdown 15
- C.3 Model Scaling Detailed Results . . 15
- C.4 Additional Per-Dataset Strategies . 15
- C.5 Best Discovered Strategy Configurations 15
- C.6 Capacity Guidebook Analysis . . 15

D Further Analysis of the Main Results **16**
- D.1 Matched-Budget Comparison with the Skill-Based Agent 17
- D.2 Detailed 8B Out-of-Memory Recovery 17
- D.3 Proposer Reasoning Trace 19
- D.4 Failure Modes Beyond Compute Limits 19

E Additional Experiments on the Public VeRL 0.7.1 Stack **19**
- E.1 Reward-Only Reasoning Ablation 19
- E.2 Backbone-Quality Ablation 20
- E.3 Poor-Default From-Scratch Ablation 20

F Search Algorithm Details **20**
- F.1 Search Loop Pseudocode 20
- F.2 UCT Computation 20
- F.3 Virtual New Child Competition . . 20

G Detailed Per-Run Results **21**
- G.1 HPO Baseline Configurations . . . 21
- G.2 Per-Run Results: Random Search 21
- G.3 Per-Run Results: Grid Search . . . 21
- G.4 Per-Iteration Results: Skill-Based LLM Agent 21
- G.5 Per-Node Results: LLMZero . . 21

H Human Knowledge Injection **21**
- H.1 Metric Descriptions 21
- H.2 Hyperparameter Descriptions . . . 21

I Agent Prompts **22**
- I.1 Proposer Agent Prompt 22
- I.2 Early Stopper Agent Prompt . . . 22

J Ethics and Artifact Documentation **22**

K Use of AI **26**

A Related Work

Multi-stage RL post-training. Progressive response length extension is the dominant pattern: DeepScaleR (Luo et al., 2025b) introduced 3-stage length scaling (8K→16K→24K), replicated by AceReason-Nemotron (Chen et al., 2025a) (4 stages to 32K), DeepCoder (Luo et al., 2025a) (code, 16K→32K), MiMo (Xiaomi et al., 2025) (32K→48K), and others (He et al., 2025; Hao et al., 2025; Chen et al., 2025b; Wan et al., 2025; Guo et al., 2025). Data difficulty staging (Chen et al., 2025a; Lai and Nissim, 2026; Song et al., 2025; Ji et al., 2025) and compression-extension cycles (Song et al., 2025; Wen et al., 2025) provide complementary patterns, while most of them hold learning rate, KL coefficient, temperature, and batch size constant across stages, leaving most of the hyperparameter space unexplored at transitions.

Adaptive training and HPO. Population-based training (PBT) (Jaderberg et al., 2017) is the closest methodological ancestor: it also discovers hyperparameter schedules during training by evolving a population of configurations. The key differences are: (1) PBT transitions via scalar fitness ranking and random perturbation, while LLMZERO diagnoses specific pathologies and proposes coordinated interventions; (2) PBT requires a population (typically 10–80 parallel workers), while LLMZERO operates sequentially with checkpoint reuse under severe budget constraints; (3) PBT's output is an opaque schedule, while LLMZERO's diagnostic analysis produces interpretable, human-readable diagnoses and a candidate design heuristic (§4.3.2), scoped to our evaluated setting. PBT excels in GPU-rich regimes where broad parallel exploration is cheap; even a minimal population of 8 workers would require 256 concurrent A100 GPUs (8×32 GPUs per training run), placing it beyond our compute budget. Random search (Bergstra and Bengio, 2012), Bayesian optimization (Snoek et al., 2012), and Hyperband (Li et al., 2018) search over static configurations without adapting within a training run. ASHA (Li et al., 2020) likewise allocates budget across static configurations via early stopping. We view these methods as complementary to and composable with LLMZERO rather than as pure competitors: the LLM proposer could replace PBT's random perturbation with dynamics-aware coordinated proposals, or steer ASHA's sampling toward promising regions, which is left to future work. LLMZERO searches over configuration *sequences* conditioned on training dynamics, staging parameters the literature holds constant with non-monotonic trajectories.

Agentic ML automation. Several concurrent systems apply LLM agents with tree-structured exploration to ML automation. SELA (Chi et al., 2024) uses MCTS for ML pipeline configuration; AIDE (Jiang et al., 2025) applies tree search to data science competitions; MLZero (Fang et al., 2025) provides end-to-end automation across modalities; and AlphaEvolve (Novikov et al., 2025) applies evolutionary search to code. LLMZERO targets a fundamentally different search space: RL post-training trajectories where (1) each evaluation costs much more GPU time, imposing severe budget constraints; (2) nodes are not independent solutions but training *phases* that compose via checkpoint resumption into multi-stage strategies; (3) the search must reason about non-stationary training dynamics (KL divergence spikes, model collapse, reward stagnation, etc.) rather than static metrics; and (4) the proposer must make coordinated multi-dimensional hyperparameter changes conditioned on the observed training state. These challenges motivate our dynamics-aware proposal mechanism and agentic early stopping.

Our contributions to the search process are: redefining nodes as training phases with checkpoint composition (§3.3), dynamics-aware multimodal proposals (§3.4), agentic early stopping (§3.5), and forced from-scratch injection (§3.3). The UCT value function with virtual child competition is adopted from prior work. Tree-of-Thought (Yao et al., 2023) and RAP (Hao et al., 2023) apply tree search at inference time where simulations are cheap; LLMZERO applies it at training time where each node requires hours of GPU compute.

While our approach focuses on optimizing RL training trajectories, a concurrent line of work shifts the focus of agentic ML automation toward autonomous data collection and curation. For instance, PostTrainBench (Rank et al., 2026) evaluates agents on their ability to autonomously gather and curate external data to optimize the post-training phase of base LLMs. Similarly, the Data-Master (Du et al., 2026) framework isolates the data engineering process, using tree-structured search and cumulative memory to let agents discover, clean, and compose datasets without altering the underlying learning algorithm. Exploring a related automated curation loop, Curation-Bench (Kang et al.,

2026) demonstrates that properly scaffolded agents can autonomously compose highly efficient data-selection policies that outperform standard baselines. These data-centric approaches complement our dynamics-aware search by targeting dataset optimization rather than training trajectory search.

LLM post-training methods. Current LLM pipelines utilize a variety of optimization algorithms for RL training, including PPO (Schulman et al., 2017), DPO (Rafailov et al., 2024), GRPO (Shao et al., 2024), GSPO (Zheng et al., 2025), etc. LLMZERO does not introduce a new alignment objective; instead, it automates the *training strategy* required to effectively deploy them. We demonstrate the efficacy of our approach specifically using GRPO, leaving its application to other algorithms for future work.

B Experimental Setup Details

B.1 Task Details

Table 4 summarizes the four evaluation tasks. All datasets are uniformly subsampled to 5,000 train, 500 validation, and 500 test examples. The dynamic orchestration workflow automatically designs a task-specific reward function for each dataset.

All datasets use fixed, deterministic splits with subsampled train ($\leq$5,000), validation ($\leq$500), and test ($\leq$500) sets. Base model performance (0.6B and 4B columns) is measured via greedy decoding (pass@1, temperature=0) with extended thinking and max response length=8192 on 2 nodes $\times$ 8 A100 40G GPUs.

B.2 Baseline Configurations

Practitioner baseline. A carefully tuned general-purpose GRPO recipe for Qwen3 (on 8x A100 40G GPUs), developed through internal iteration on separate tasks (e.g., math reasoning) and applied without task-specific modification. Single static configuration ($L = 1$).

Random search. 8 trials with configurations sampled from: learning rate $\sim$ LogUniform(1e-5, 1e-4), KL coefficient $\sim$ LogUniform(1e-5, 1e-3), temperature $\sim$ Uniform(0.6, 1.2), clip ratio $\sim$ Uniform(0.15, 0.35), batch size $\in \{64, 128, 256\}$, LoRA rank $\in \{16, 32, 64, 128\}$, rollout count $\in \{6, 8, 12\}$, epochs $\in \{3, 5\}$. Each trial runs to completion without early stopping.

Skill-based LLM agent. An autonomous LLM agent (Claude Opus 4.6) built on the same training infrastructure to LLMZERO (VeRL, reward functions, hyperparameter space). Unlike LLMZERO's fixed workflow where each stage has a deterministic prompt template, the iterative agent uses a skill-based general workflow: the LLM autonomously plans and orchestrates each iteration, invoking skills for dataset preparation, reward design, job submission, metric diagnosis, and checkpoint resume. This generality makes it more flexible but less token-efficient (73$\times$ higher API cost) since the LLM must maintain full context across all decisions. It can stop training at any time and resume from any previous checkpoint, without explicit tree search or visual reasoning.

B.3 Compute Budget Fairness

Random and grid search each run 8 full-length training runs to completion and achieve similar total GPU-hours to LLMZERO. Both LLMZERO and the skill-based LLM agent have a maximum of 16 iterations, but the skill-based agent is limited to less than 700 GPU-hours of total runtime due to its significant API cost (Table 5). This budget is sufficient for convergence: the agent does not force restarts from scratch, and its validation scores begin to plateau or decrease near the end of its time limit (Table 20, Figure 2). Notably, LLMZERO's best discovered strategy on all four tasks originates from the root node (the practitioner default configuration), indicating that the default is a strong starting point and that forced from-scratch injection, while necessary for robustness, was not the source of the best strategies in these experiments.

B.4 API Cost

Table 5 compares API costs between LLMZERO and the skill-based LLM agent. The fixed workflow with structured prompts at each stage consumes 73$\times$ less total API cost than the agent's autonomous orchestration, which must maintain full conversation context across all decisions.

B.5 Model and Infrastructure

All experiments use Qwen3-4B as the base model with LoRA. Training uses a modified version of VeRL (for better LoRA support, etc.) on Ray clusters deployed on AWS EKS with 4 to 8$\times$A100 40G nodes. The scaling experiment (Table 7) additionally evaluates Qwen3-0.6B, 1.7B, and 8B.

Table 4: Evaluation tasks. All tasks train with GRPO via VeRL. For ChemCoT we report the average over subtasks in this table.

Dataset	Domain	Answer format	Metric	Train	0.6B	4B
ChemCoT	Chemistry (19 subtasks)	Mixed (SMILES, MCQ)	Task-specific	5,000	15.4	14.6
PaperSearchQA	Biomedical QA	Short text	Exact match	5,000	11.6	31.6
SSMR-Bench	Music theory	MCQ (A to D)	EM accuracy	5,000	32.4	51.4
WildSci	Multi-discipline science	MCQ (A to J)	EM accuracy	5,000	29.4	53.6

Table 5: LLM API cost comparison (ratios from unrounded costs). LLMZERO's structured pipeline uses 73× less API cost than the skill-based LLM agent.

Dataset	LLMZERO ($)	LLM Agent ($)	Ratio
ChemCoT	14	639	44×
PaperSearchQA	11	635	58×
WildSci	15	1,125	74×
SSMR-Bench	8	1,146	144×
Total	**48**	**3,545**	**73×**

B.6 LLMZERO Configuration

$C = 1.414$, $T = 0.3$, $w_f = 0.5$, $w_e = 0.3$, $o_f = 2$, max evolve children = 2, max debug children = 3, max debug depth = 5, $\rho_{\min} = 0.2$, early stopping interval = 900s. LLM backbone (main results): Claude Opus 4.5 for the proposer and the early stopper; the skill-based LLM agent uses Claude Opus 4.6 (Appendix B.7). The framework is backbone-agnostic, but stronger reasoning models are preferred (Appendix E.2). The additional public-stack experiments in Appendix E use Claude Opus 4.8 as the default backbone.

B.7 Skill-Based LLM Agent

The skill-based LLM agent uses Claude Opus 4.6 as an autonomous orchestrator with unrestricted tool access. Rather than a fixed pipeline, the agent is equipped with 8 *skills*, which are natural language instruction sets that the LLM invokes as needed:

1. `prepare-dataset`: Download and convert data to VeRL parquet format
2. `define-reward`: Analyze dataset and write a `compute_score()` reward function
3. `validate-run`: Pre-flight evaluation on a sample
4. `generate-config`: Write a full VeRL sweep configuration
5. `download-model`: Download the base model
6. `submit-training`: Generate and submit SLURM jobs
7. `check-training`: Monitor metrics, diagnose training health, recommend action
8. `gather-results`: Parse outputs and write a report

The agent's optimization loop proceeds as: (1) submit a training job, (2) poll metrics at 5–30 minute intervals, (3) perform a 14-parameter diagnostic analysis producing a per-parameter verdict (KEEP/INCREASE/DECREASE) based on observed KL divergence, gradient norms, clip ratios, and validation trends, (4) decide whether to continue, early-stop, tune-and-resume from the best checkpoint, or restart from scratch.

The agent can also be coupled with LLMZERO to form an end-to-end training experience with static workflow as search backend.

Key differences from LLMZERO. The agent maintains full conversation context across all decisions (leading to long token histories), plans its own workflow (may skip or reorder stages), and tends to always resume from the single best checkpoint in a linear chain. It analyzes only numerical metrics (no visual training curves). These design choices make it more flexible than LLMZERO's fixed harness but 73× less token-efficient.

Budget limitation. Due to high API cost ($635–1,146 per task), the agent was limited to 6–9 training iterations (488–709 GPU-hours) rather than the full 16-iteration budget allocated to LLMZERO. This limitation is inherent to the agent's design: autonomous orchestration requires maintaining full conversation context, making it 73× more expensive in API cost overall than LLMZERO's fixed prompts. A budget-matched comparison at equal GPU-hours would require either reducing the agent to 1–2 iterations or spending $10K+ per task, neither of which yields a meaningful evaluation. Despite this handicap, it achieves competitive results

(Table 1), confirming that LLM reasoning about training dynamics is broadly effective. The advantage of LLMZERO comes from its tree structure and fixed harness rather than from a fundamentally different reasoning capability.

C Additional Results and Analysis

C.1 Search Convergence

Figure 5 shows best-so-far validation score vs. search iteration for all 4 tasks. LLMZERO surpasses the practitioner baseline early in the search and continues improving throughout the budget.

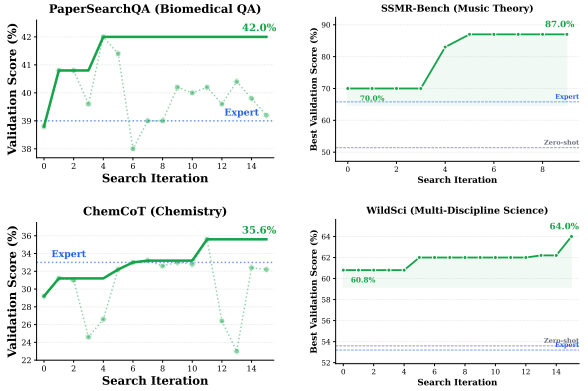

Figure 5: Best-so-far validation score vs. search iteration. LLMZERO surpasses the practitioner baseline early in the search and continues improving throughout the budget.

C.2 ChemCoT Per-Subtask Breakdown

Table 6 reports per-subtask test accuracy for ChemCoT.

C.3 Model Scaling Detailed Results

Table 7 reports per-subtask results for the scaling analysis on SSMR-Bench.

C.4 Additional Per-Dataset Strategies

We describe the two per-dataset strategies deferred from §4.3.1; full per-phase configurations for all four tasks appear in Tables 8–11.

PaperSearchQA (Biomedical QA). The best strategy is a 4-phase chain (Figure 3, test=42.6%, +11.0 pp over the base model). LR and temperature are progressively tightened through Phases 2–3 (val stabilizes at 40.8%), then the proposer diagnoses stagnation (near-zero clip ratio, low gradient norms) and reverses course at Phase 4: LR doubles, temperature increases, and batch size decreases to break the plateau (val=42.0%). The KL coefficient increases monotonically throughout ($0.001 \rightarrow 0.01$), unlike the non-monotonic trajectories on other tasks.

WildSci (Multi-Discipline Science). The best strategy is a 4-phase chain (Figure 3, test=58.5%). After aggressive LR scaling in Phase 2 triggers a KL divergence spike, the system tightens constraints in Phase 3. This intervention causes an entropy collapse. During this collapse, the validation score increases slightly, but the hidden test score drops. To recover entropy, Phase 4 relaxes the KL penalty, lowers the LR, and raises both the temperature and the clip ratio. This successfully recovers the hidden test performance, though it does not fully surpass the Phase 2 peak due to the negative effects of Phase 3. Noticeably, the validation score continued to rise even as test performance degraded during the entropy collapse, which suggests that monitoring comprehensive training dynamics is more robust than optimizing solely for the validation score.

C.5 Best Discovered Strategy Configurations

Tables 8–11 detail the full hyperparameter configuration at each phase of the best discovered strategy for each task. For each phase, we report the node ID in the search tree, the training step range, the proposer's diagnosis that triggered the transition, and the complete configuration.

C.6 Capacity Guidebook Analysis

Comparing the Capacity Guidebook to the full SSMR transfer (Table 3) isolates the contribution of regularization oscillation versus pure capacity expansion.

WildSci. Both schedules converge to near-identical performance (58.3% vs. 58.4% vs. LLMZERO's 58.5%), confirming that expanded reasoning capacity, rather than hyperparameter oscillation, drives improvement on this task.

ChemCoT. The SSMR transfer (41.3%) substantially outperforms the Capacity Guidebook (36.6%), indicating that LR/KL oscillation provides +4.7 pp beyond pure capacity scaling, consistent with the KL divergence spike diagnosis in §4.3.1.

PaperSearchQA. Both fixed schedules underperform the static practitioner (37.8% and 36.2% vs. 39.0%), confirming that this task's progressive-

Table 6: ChemCoT per-subtask test accuracy (%) for Qwen3-4B (pass@1, rl=8192), the first training run (Node 0), and the best discovered strategy (Node 11, 5-phase adaptive). Subtasks sorted by Node 11 accuracy. Nine subtasks scoring 0% across all conditions are omitted (all `mol_opt_*`, `rxn_retro`, `rxn_nepp`, `rxn_mechanism`). *Note that the average number here refers to average over subtasks which is different from the average over domains in main table.*

Category	Subtask	Base	Node 0	Node 11
Mol. Understanding	fg_count	75.9	82.8$_{(+6.9)}$	**96.6**$_{(+20.7)}$
	ring_count	16.1	80.6$_{(+64.5)}$	**93.5**$_{(+77.4)}$
	ring_system	70.0	83.3$_{(+13.3)}$	**86.7**$_{(+16.7)}$
	equivalence	37.0	**55.6**$_{(+18.6)}$	**55.6**$_{(+18.6)}$
	murcko	3.3	3.3$_{(+0.0)}$	**16.7**$_{(+13.4)}$
Mol. Editing	substitution	0.0	31.0$_{(+31.0)}$	**58.6**$_{(+58.6)}$
	deletion	20.7	**37.9**$_{(+17.2)}$	34.5$_{(+13.8)}$
	addition	3.4	0.0	**6.9**$_{(+3.5)}$
Reaction	reagent/catalyst	11.5	72.1$_{(+60.6)}$	**90.2**$_{(+78.7)}$
	forward synth. byproduct	0.0	**2.6**$_{(+2.6)}$	**2.6**$_{(+2.6)}$
Macro-avg (all 19 subtasks)		12.5	23.6$_{(+11.1)}$	**28.5**$_{(+16.0)}$

Table 7: Model scaling analysis on SSMR-Bench: per-subtask test accuracy (%) at the best validation node. Subscripts show gain over the base model. **Bold**: best per subtask per model.

Model	Method	Scl	Bea	Cho	Int	Avg
Qwen3-0.6B	Qwen3	33.6	30.4	39.2	26.4	32.4
	Practitioner	53.6	75.2	37.6	45.6	53.0
	LLMZERO	**95.2**$_{(+61.6)}$	**82.4**$_{(+52.0)}$	**60.0**$_{(+20.8)}$	**52.0**$_{(+25.6)}$	**72.4**$_{(+40.0)}$
Qwen3-1.7B	Qwen3	27.2	31.2	36.0	32.0	31.6
	Practitioner	56.8	50.4	50.4	**51.2**	52.2
	LLMZERO	**77.6**$_{(+50.4)}$	**69.6**$_{(+38.4)}$	**55.2**$_{(+19.2)}$	47.2$_{(+15.2)}$	**62.4**$_{(+30.8)}$
Qwen3-4B	Qwen3	60.0	44.8	50.4	50.4	51.4
	Practitioner	76.8	60.0	65.6	60.8	65.8
	LLMZERO	**94.4**$_{(+34.4)}$	**81.6**$_{(+36.8)}$	**77.6**$_{(+27.2)}$	**75.2**$_{(+24.8)}$	**82.2**$_{(+30.8)}$
Qwen3-8B	Qwen3	59.2	56.0	48.8	46.4	52.6
	Practitioner			*failed (OOM)*		
	LLMZERO	**96.8**$_{(+37.6)}$	**88.0**$_{(+32.0)}$	**79.2**$_{(+30.4)}$	**70.4**$_{(+24.0)}$	**83.6**$_{(+31.0)}$

tightening dynamic cannot be captured by any fixed multi-stage recipe.

These results support the candidate design heuristic: capacity parameters should accumulate monotonically, but the task-specific LR and KL trajectories that LLMZERO discovers are essential for realizing the full benefit of multi-stage training.

Transfer caveats. Both the SSMR transfer and the Capacity Guidebook benefit from all tasks sharing the same subsampled dataset size (5,000 training examples), which produces similar steps-per-epoch and possibly comparable training dynamics timelines. Transferring fixed schedules between datasets of substantially different sizes may require recalibrating transition points, as the step at which the model saturates its current response budget depends on dataset complexity and size. This is an additional advantage of adaptive methods: they discover appropriate transition points from observed dynamics regardless of dataset scale.

D Further Analysis of the Main Results

The analyses below further examine our main-paper results (internal VeRL build; Qwen3-4B, except the 8B recovery, which comes from the scaling analysis of §4.4). They introduce no new training runs and are separate from the public VeRL 0.7.1 suite of Appendix E.

Table 8: Best discovered strategy for **ChemCoT** (5-phase, Node path: 0→2→3→5→11). Node 2 resumes from Node 1's checkpoint (Node 1 failed but produced a valid checkpoint). Final val=35.6%, test=28.5% (macro-avg 19 subtasks).

Phase	Node / Steps	Proposer Diagnosis	Configuration
1	Node 0, steps 0–59	(Initial run)	LR=5e-5, KL=0.001, T=1.0, clip=0.28, batch=128, rollout=8, resp=6144, epochs=1
2	Node 2, steps 60–79	Under-exploring: low reward variance under default constraints	LR=5e-5, KL=0.001, T=0.85, clip=0.3, adv_norm=true
3	Node 3, steps 80–116	KL divergence spike: 16× KL loss spike, response length inflating (1630→2278 tokens) without val improvement	LR=2.5e-5, KL=0.005 (5× increase), T=0.7, clip=0.25
4	Node 5, steps 117–119	Response truncation: clip ratio rising (3%→8%) indicating output capacity exhaustion	LR=2e-5, KL=0.003, resp=7168 (+1024), clip=0.28
5	Node 11, steps 120–180	Low gradient signal: gradient norms <0.001, validation flat at 32.8%	LR=3e-5 (↑), KL=0.005, T=0.8, rollout=12 (↑), batch=96 (↓), clip=0.25

Table 9: Best discovered strategy for **PaperSearchQA** (4-phase, Node path: 0→1→2→5). Final val=42.0%, test=42.6%.

Phase	Node / Steps	Proposer Diagnosis	Configuration
1	Node 0, steps 0–99	(Initial run)	LR=5e-5, KL=0.001, T=1.0, clip=0.28, batch=128, epochs=3
2	Node 1, steps 100–119	Noisy updates: high variance in reward signal, LR too aggressive for task difficulty	LR=2.5e-5, KL=0.002, T=0.9, clip=0.28, algo_kl=0.002, epochs=5
3	Node 2, steps 120–139	Continued noise: val improvement slowing, further constraint needed	LR=1e-5 (↓), KL=0.005 (↑), T=0.7 (↓), clip=0.25, algo_kl=0.005, epochs=6
4	Node 5, steps 140–312	Validation plateau: val flat at 40.8%, near-zero clip ratio, low gradient norms	LR=2e-5 (↑), KL=0.01 (↑), T=0.8 (↑), clip=0.3 (↑), batch=96 (↓), algo_kl=0.01

D.1 Matched-Budget Comparison with the Skill-Based Agent

The skill agent's 6–9 iterations follow from its 73× higher API cost (Table 5), not a design choice. Capping LLMZERO at its first 8 iterations (within that range) and scoring each method at its best-so-far validation node (per-node tables in Appendix G), LLMZERO matches or exceeds the skill agent on all four tasks (Table 12); on ChemCoT it still beats the skill agent (37.4 vs. 37.0) but ranks second behind random search. The iteration gap thus does not explain its advantage. We keep the API-cost limit explicit rather than claim a GPU-matched win (a GPU-matched skill run would exceed $10,000/task in API); the skill agent shares our proposer implementation and is part of our contribution, not a fully external baseline.

D.2 Detailed 8B Out-of-Memory Recovery

From the run logs (Qwen3-8B, SSMR-Bench): the practitioner default failed at vLLM rollout-engine initialization, before any training step (*"No available memory for the cache blocks..."*). With `gpu_memory_utilization`=0.4 and `tensor_model_parallel_size`=1, the 8B weights, FSDP actor/reference parameters, and optimizer state left too little memory for vLLM's KV-cache at the 10,240-token max sequence (4,096 prompt + 6,144 response).

Table 10: Best discovered strategy for **SSMR-Bench** (4-phase, Node path: 0→1→4→5). Final val=87.0%, test=82.2%.

Phase	Node / Steps	Proposer Diagnosis	Configuration
1	Node 0, steps 0–19	(Initial run)	LR=5e-5, KL=0.001, clip=0.28, T=1.0, resp=6144, epochs=1
2	Node 1, steps 20–39	Fast initial convergence: model learning MCQ pattern quickly, apply conservative tuning	LR=3e-5 (↓), KL=0.002 (↑), clip=0.25, grad_clip=0.5, adv_norm=true, T=1.1, epochs=2
3	Node 4, steps 40–139	Validation regression: val regressed 70.0%→67.2% under conservative hyperparameters	LR=5e-5 (restored), KL=0.001 (relaxed), clip=0.30, T=1.1, epochs=4
4	Node 5, steps 140–200	Convergence stabilization: val jumped to 83.0%, now fine-tune with expanded capacity	LR=3e-5 (↓), KL=0.002 (↑), resp=7168 (+1024), T=1.0, clip=0.25, epochs=6

Table 11: Best discovered strategy for **WildSci** (4-phase, Node path: 0→5→13→15). Final val=64.0%, test=58.5%.

Phase	Node / Steps	Proposer Diagnosis	Configuration
1	Node 0, steps 0–99	(Initial run)	LR=5e-5, KL=0.001, T=1.0, clip=0.28, resp=6144
2	Node 5, steps 100–119	Slow progress: multi-domain task needs stronger signal, try aggressive exploration	LR=1e-4 (↑ 2×), KL=0.002, T=0.9, clip=0.25, adv_norm=true
3	Node 13, steps 120–139	KL divergence rising: KL loss rising without val improvement, model collapse from aggressive LR	LR=5e-5, KL=0.005 (↑), T=0.85, clip=0.22, algo_kl=0.002
4	Node 15, steps 140–195	Model collapse: entropy at ∼0.2 (vs. ∼0.7–0.8 healthy), policy distribution narrowed prematurely	LR=3e-5, KL=0.002 (↓), T=0.95 (↑), clip=0.28 (↑), clip_low=0.15

Table 12: Matched refinement-iteration budget: test score (%) at the best-so-far validation node, with LLMZERO capped at its first 8 search iterations (within the skill agent's 6–9 range). WildSci here reads 58.6 from the per-node table; cf. 58.5 for the full 16-iteration run in Table 1.

Task	Skill-based agent	LLMZERO (first 8 iters)
ChemCoT	37.0	37.4
PaperSearchQA	40.2	42.6
SSMR-Bench	80.0	82.2
WildSci	56.6	58.6

LLMZERO's error analyzer diagnosed this and recovered autonomously by raising `gpu_memory_utilization` to 0.6 and `tensor_model_parallel_size` to 2 and enabling `enforce_eager`, plus two secondary fixes (raising `max_num_batched_tokens` to 10,240 under chunked prefill, and reverting an FSDP2/DTensor incompatibility from parameter offloading), so the fix required reasoning about the KV-cache and FSDP memory layout, not a single toggle. The best 8B configuration reached 83.6% test versus 52.6% for the base model (Table 13, matching Table 7). As in §4.4, we do not claim OOM recovery as a fundamental capability (a practitioner could fix it manually), only that LLMZERO navigated it autonomously.

Table 13: Best discovered Qwen3-8B configuration on SSMR-Bench (per-subtask test %).

Subtask (SSMR-Bench, Qwen3-8B)	LLMZERO best config
Scale	96.8
Beat	88.0
Chord	79.2
Interval	70.4
Test average	83.6

D.3 Proposer Reasoning Trace

This SSMR-Bench trace shows coordinated, diagnosis-conditioned reasoning that random search cannot replicate. At Node 1 the proposer tightened five parameters at once (lower LR, doubled KL, narrower `clip_ratio_high`, advantage normalization, halved `grad_clip`) to stabilize near the optimum; this over-constrained learning and regressed validation from 70.0% to 67.2%. At Node 4 it diagnosed and reversed that decision:

> *"The training shows clear signs of plateauing with validation score stuck at 0.67 since step 25, while the best historical run achieved 0.70. The KL loss is steadily increasing (0.001 -> 0.012) indicating policy drift from the reference, but this isn't translating to validation gains. The clip ratio decreased significantly (0.11 -> 0.04), suggesting the policy updates became more conservative over time... The gradient norms remain stable (~0.0014–0.0019), so training mechanics are healthy but the learning signal appears exhausted."*

It then loosened five parameters together, each with a causal justification: raising LR (low gradient norms plus a plateau imply too-conservative steps), widening `clip_ratio_high` (updates had grown too conservative), raising temperature (to counter entropy decline), and lowering both the KL loss and reward-side KL coefficients (the penalty was over-constraining useful updates), driving validation from 67.2% to 83.0%. Random search samples configurations independently and cannot condition such a coordinated loosening on a specific diagnosis, nor reverse a specific earlier over-constraint.

D.4 Failure Modes Beyond Compute Limits

Beyond compute limits, LLMZERO has two failure modes. (1) The proposer can misinterpret a hyperparameter, metric, or dynamics signal when the grounding knowledge is absent, which is why we inject knowledge (Appendix H); e.g., LLMs routinely confuse PPO policy clipping with the response-length truncation ratio (`response_length/clip_ratio`), so on a new framework or unfamiliar metrics high-quality descriptions are essential. (2) A base-model capability boundary caps what any schedule can reach: on ChemCoT, nine molecular-optimization and reaction subtasks score 0% for every method, as valid SMILES generation is a capability the 4B base model lacks (§4.3.1). Adaptive scheduling optimizes *how* to train but cannot elicit a rollout the model cannot produce.

E Additional Experiments on the Public VeRL 0.7.1 Stack

All experiments here use the fully public VeRL 0.7.1 release, so they also re-confirm our main claims on a public stack, independent of the internal build. Setup: Qwen3-0.6B (LoRA rank 64), SSMR-Bench subsampled to 2,500 / 200 / 200 (train/val/test), 16 LLMZERO MCTS iterations on one 8-GPU node, Claude Opus 4.8 backbone; we report test accuracy (%) at the best-validation node, averaged over the four SSMR-Bench subtasks (Scl=scale, Bea=beat, Cho=chord, Int=interval). The full system reaches 61.5% versus 44.0% for default GRPO (4 epochs, no search) and 30.5% for the base model (Table 14). *These runs use a smaller dataset (and model) than the main experiments and serve as an extended ablation, so their absolute numbers are not directly comparable to the main results.*

Table 14: Ablation and backbone suite on the public VeRL 0.7.1 stack (Qwen3-0.6B, SSMR-Bench). Test accuracy (%) at the best-validation node, averaged over four subtasks; Val is the aggregate validation score at that node.

Condition	Test	Scl	Bea	Cho	Int	Val
Base model (untrained)	30.5	34	26	30	32	∼25
Default GRPO, 4 ep. (no search)	44.0	66	58	34	18	52.0
LLMZERO full system (Opus 4.8)	**61.5**	78	78	48	42	73.5
Ablation: reward-only signal	49.5	64	66	42	26	56.0
Backbone: Sonnet 4.6	55.5	84	64	42	32	62.5
Backbone: Haiku 4.5	39.5	54	48	40	16	49.0

E.1 Reward-Only Reasoning Ablation

To isolate the LLM's reasoning from the tree-search machinery, we give the proposer and early stopper only the scalar reward, removing every diagnostic signal they normally read (KL, entropy, gradient norms, clip ratios, response-length dynamics) while holding all else fixed. Test mean drops from 61.5% to 49.5% (Table 14), a 12-point loss. Since removing the proposer entirely would collapse the system into random/grid search, this is the cleanest way to isolate the reasoning content; it complements the component-level ablations of Table 2.

E.2 Backbone-Quality Ablation

Varying only the proposer/early-stopper backbone (all else fixed), test accuracy rises monotonically with reasoning capability: Haiku 4.5 39.5%, Sonnet 4.6 55.5%, Opus 4.8 61.5% (Table 14). The weakest backbone falls below the no-search default GRPO (44.0%) while stronger ones clear it widely; were the budget alone responsible, a weaker reasoner would not regress to the static-training band. Reasoning quality, not the tree machinery alone, is thus a primary driver of search quality. The framework is backbone-agnostic but favors stronger reasoners.

E.3 Poor-Default From-Scratch Ablation

From-scratch injection (§3.3) is regime-dependent: it looks inert when the default is already strong, as on all four tasks, where the best strategy comes from the root subtree. Under a deliberately weak default (KL=10^{-2}), the best node reaches 56.1% test and descends from an injected from-scratch node, versus 51.5% for the best root-subtree descendant (a 4.6-point gap); recovery takes several iterations as the proposer walks $10^{-2} \to 5 \times 10^{-3} \to 2 \times 10^{-3}$ to a healthy range. This positions the mechanism as robustness insurance, with $\rho_{\min}$ a tunable exploration knob.

F Search Algorithm Details

While the UCT computation and virtual child competition mechanisms are adopted from prior work (reproduced here for completeness), we introduce the failure subtree pruning (§3.2) to improve search efficiency and forced from-scratch injection mechanism (§3.3) to maintain exploration diversity. As search optimization is not the primary focus of this paper, we leave the design of more sophisticated search algorithmsthat could further improve performance, particularly those tailored for budget constraints (Fang and Wang, 2026) or asynchronous execution, to future work.

F.1 Search Loop Pseudocode

Algorithm 1 summarizes the main loop. At each iteration, UCT selection traverses the tree to choose a parent node for expansion. If the selected parent failed, an error analyzer diagnoses the failure and proposes a fix; otherwise, the proposer agent analyzes the parent's training dynamics and proposes a new configuration with a checkpoint to resume from. The resulting child node is executed as a training job, monitored by the agentic early stopper at fixed intervals. Upon completion (or early termination), the best validation score is back-propagated up the tree and terminal subtrees are pruned. The final output is the scratch-to-leaf path with the highest validation score, interpreted as a multi-stage adaptive strategy.

F.2 UCT Computation

We integrate expansion into selection via a *virtual new child* that competes against existing children at every internal node. At node p with existing children $\{c_1, \ldots, c_k\}$:

$$\mathrm{UCT}(c_i) = Q(c_i) + C\sqrt{\frac{\ln N(p)}{N(c_i)}}, \tag{5}$$

$$\mathrm{UCT}(\text{new}) = Q_{\text{prior}}(p) + C\sqrt{\frac{\ln N(p)}{N_{\text{fair}}}}, \tag{6}$$

where $Q_{\text{prior}}(p)$ is the parent's own normalized score (encoding the prior belief that a new child will perform similarly to its parent) and $N_{\text{fair}} = N(p)/(k+1)$ gives the virtual child a fair share of the parent's visit budget.

The exploitation term $Q(c)$ uses min-max normalization followed by exponential shaping for scale invariance:

$$\hat{s} = \frac{s - s_{\min}}{s_{\max} - s_{\min}}, \qquad f_T(\hat{s}) = \frac{e^{\hat{s}/T} - 1}{e^{1/T} - 1}, \tag{7}$$

where T is a temperature parameter (default 0.3). The full exploitation term combines three signals:

$$Q(c) = \frac{v_{\text{val}}}{v_{\text{total}}} \cdot f_T(\bar{s}_c) - w_f \cdot \frac{\max(0,\, v_{\text{fail}} - o_f)}{v_{\text{total}}} - w_e \cdot \frac{v_{\text{early}}}{v_{\text{total}}}, \tag{8}$$

where v_{val}, v_{fail}, v_{early}, v_{total} are validated, failed, early-stopped, and total visit counts; $\bar{s}_c$ is the average normalized score of validated descendants; $w_f = 0.5$ and $w_e = 0.3$ are penalty weights; and o_f (default 2) forgives the first o_f failures before penalizing.

F.3 Virtual New Child Competition

At each internal node p during selection traversal:

1. Compute UCT for all existing non-terminal children $\{c_1, \ldots, c_k\}$ (Eq. 5).

2. Compute UCT for the virtual new child (Eq. 6) with $Q_{\text{prior}} = f_T(\hat{s}_p)$ and $N_{\text{fair}} = N(p)/(k+1)$.

3. If UCT(new) $>$ $\max_i \text{UCT}(c_i)$ **and** $k < k_{\max}$: expand (create new child at p).

4. Otherwise: descend into $\arg\max_i \text{UCT}(c_i)$ and repeat.

This mechanism naturally adapts breadth vs. depth: when children underperform their parent, the virtual child's prior wins, triggering exploration of a new transition from the same checkpoint.

G Detailed Per-Run Results

This section reports the full hyperparameter configuration and performance for every run across all methods and tasks.

G.1 HPO Baseline Configurations

Practitioner baseline. Table 15 reports the practitioner configuration, a carefully tuned general-purpose GRPO recipe applied identically to all tasks.

Table 15: Practitioner baseline configuration (applied to all tasks without modification).

Parameter	Value
Learning rate	5e-5
KL coefficient	0.001
Temperature	1.0
Clip ratio (high)	0.28
Train batch size	128
LoRA rank / alpha	64 / 64
Rollout count (n)	8
Epochs	1
Response length	6144
Gradient clip	1.0
Weight decay	0.01
Advantage normalization	false

Capacity Guidebook. Table 16 reports the 3-phase capacity-scaling schedule. All hyperparameters not listed remain at practitioner defaults (Table 15). Phase durations are inspired by transition points observed in LLMZERO's discovered strategies.

Grid search. All grid runs use the practitioner defaults except for two swept parameters: LR $\in$ {1e-5, 3e-5, 5e-5, 1e-4} $\times$ LoRA rank $\in$ {64, 128} (8 configurations per task). **Grid runs additionally use epochs=5 and response length=8192**.

Table 16: Capacity Guidebook configuration. Progressive capacity scaling with all other hyperparameters fixed to practitioner defaults (Table 15).

Phase	Steps	Response Length	Rollout n
1	0–60	4096	6
2	60–120	6144	8
3	120–180	8192	12

Random search. Each run samples all hyperparameters independently. Table 17 reports the sampled configurations.

G.2 Per-Run Results: Random Search

Table 18 reports results for each random search trial.

G.3 Per-Run Results: Grid Search

Table 19 reports results for each grid search trial.

G.4 Per-Iteration Results: Skill-Based LLM Agent

Table 20 reports per-iteration results for the skill-based LLM agent.

G.5 Per-Node Results: LLMZERO

Tables 21–24 report per-node results for LLMZERO on all four tasks.

H Human Knowledge Injection

Even the latest LLMs frequently misinterpret domain-specific training metrics and hyperparameters in GRPO/PPO. For example, models consistently confuse PPO policy clipping with response length clipping. To ground the LLM's reasoning, we inject structured human-written descriptions for metrics and hyperparameters into the prompt. Importantly, these descriptions do *not* restrict the LLM to only modifying listed parameters; the agent can change any hyperparameter in the training configuration, including those not covered by the guide.

H.1 Metric Descriptions

Figure 6 lists the 12 metric descriptions injected into both the proposer and early stopper prompts. These address common LLM misinterpretations.

H.2 Hyperparameter Descriptions

Figure 7 provides the hyperparameter reference guide injected into the proposer prompt. Parameters are organized by functional category. The

Table 17: Random search hyperparameter configurations for all tasks. LR=learning rate, KL=KL coefficient, T=temperature, Cl=clip ratio, BS=batch size, Rk=LoRA rank, Ro=rollouts, Ep=epochs, RL=response length.

Task	Run	LR	KL	T	Cl	BS	Rk	Ro	Ep	RL
PaperSearchQA	00	2.65e-5	5.1e-5	0.98	0.17	64	64	6	3	8192
	01	5.68e-5	2.6e-4	0.61	0.26	128	128	6	3	4096
	02	1.69e-5	1.5e-4	0.65	0.30	256	16	12	3	8192
	03	1.07e-5	1.9e-5	0.96	0.22	64	128	6	5	8192
	04	5.32e-5	2.4e-4	0.70	0.24	64	32	8	5	8192
	05	8.99e-5	2.7e-4	0.66	0.32	64	128	8	5	8192
	06	1.06e-5	7.1e-4	0.85	0.21	64	32	6	5	8192
	07	6.00e-5	5.0e-4	0.83	0.26	256	64	12	3	8192
WildSci	00	2.33e-5	3.0e-4	0.71	0.26	64	64	6	3	8192
	01	1.02e-5	2.0e-5	1.02	0.19	128	32	8	3	4096
	02	7.11e-5	1.1e-4	0.64	0.28	64	64	8	5	4096
	03	2.12e-5	5.4e-4	1.06	0.28	128	32	6	5	8192
	04	2.44e-5	5.8e-5	0.84	0.24	128	128	8	5	4096
	05	1.40e-5	5.8e-4	0.78	0.24	64	16	6	3	4096
	06	6.63e-5	2.2e-4	0.88	0.27	256	128	6	5	8192
	07	4.19e-5	8.1e-4	1.08	0.18	256	32	12	5	8192
SSMR-Bench	00	6.07e-5	1.1e-4	0.80	0.16	128	32	8	5	8192
	01	4.25e-5	2.0e-5	0.95	0.26	64	128	8	3	8192
	02	6.04e-5	1.2e-5	0.84	0.34	64	64	6	3	8192
	03	2.85e-5	1.8e-4	0.92	0.22	128	64	8	5	8192
	04	3.18e-5	4.3e-5	0.85	0.17	128	128	12	5	4096
	05	5.13e-5	2.4e-4	0.94	0.33	256	16	12	3	4096
	06	1.97e-5	2.9e-5	0.68	0.17	64	64	8	5	8192
	07	1.18e-5	2.1e-4	0.76	0.31	256	64	8	3	8192
ChemCoT	00	1.83e-5	3.3e-5	0.84	0.30	64	32	6	3	4096
	01	4.71e-5	4.9e-5	0.77	0.16	128	32	6	5	4096
	02	1.26e-5	9.4e-4	1.09	0.22	256	128	8	3	8192
	03	1.78e-5	6.3e-4	1.09	0.32	64	64	6	5	8192
	04	5.40e-5	8.6e-5	0.91	0.18	256	64	6	3	8192
	05	1.43e-5	6.9e-5	1.03	0.23	64	16	6	5	4096
	06	7.83e-5	1.7e-4	1.10	0.19	64	16	6	5	4096
	07	1.31e-5	4.1e-5	1.12	0.20	128	16	12	5	4096

LLM is not restricted to modifying only these parameters; it can change any value in the training configuration. For readability, some entries in Figure 7 are compressed relative to the injected prompt; for example, the `rollout.n` entry is followed in the actual prompt by a second line, "Increase for better learning signal; decrease to save compute," so that among all tracked hyperparameters only `kl_loss_coef` and `max_response_length` carry a strictly single-directional cue. This is relevant to the directional-prompt discussion in §4.3.2.

I Agent Prompts

We provide the full proposer and early stopper prompts below. These prompts were minimally tuned: we deliberately avoided hardcoding any numeric thresholds or task-specific values, relying instead on the LLM's reasoning to interpret metrics in context. This design leaves substantial room for improvement through prompt engineering, and we expect that more carefully crafted prompts could further improve search efficiency.

I.1 Proposer Agent Prompt

The proposer receives the previous training configuration (as YAML), step-level metric summaries (text and/or plots), and produces a diagnosis with hyperparameter suggestions. The template (Figure 8) is instantiated with run-specific data at each iteration; placeholders in `{braces}` are filled dynamically.

I.2 Early Stopper Agent Prompt

The early stopper receives comparison plots (current run in blue vs. best run in green) and decides whether to continue or stop. The prompt template is shown in Figure 9.

J Ethics and Artifact Documentation

Potential risks. LLMZERO automates hyperparameter search for RL post-training, which could lower the barrier to fine-tuning language models for harmful purposes. However, the system requires substantial compute, limiting misuse to well-resourced actors who already have access to equivalent capabilities.

Artifact licenses. All artifacts are used under their respective open-source licenses.

Artifact	License
Qwen3 (0.6B–8B)	Apache 2.0
ChemCoTBench	CC BY 4.0
PaperSearchQA	MIT
SSMR-Bench	MIT
WildSci	CC BY 4.0
VeRL	Apache 2.0
Ray	Apache 2.0

Metric Descriptions (injected into both proposer and early stopper prompts)

`actor/entropy`	Policy entropy measuring exploration. Healthy: dropping with rising rewards. Problem: both dropping (losing generality without gains).
`actor/kl_loss`	KL divergence loss measuring policy divergence from old policy. Should remain small and stable.
`actor/ppo_kl`	PPO KL divergence. **Critical:** if ppo_kl spikes AND rewards drop afterward, training has collapsed.
`actor/pg_loss`	Policy gradient loss (primary training signal). Should generally decrease as policy improves.
`actor/pg_clipfrac`	PPO policy clipping fraction (upper). Ratio of updates hitting clip_ratio_high. High (>0.3) = many updates being prevented. **Unrelated to response_length/clip_ratio.**
`actor/pg_clipfrac_lower`	PPO policy clipping fraction (lower). Shows how often PPO constrains updates. **Unrelated to response_length/clip_ratio.**
`actor/grad_norm`	Gradient norm magnitude. Very high = instability; very low = vanishing gradients.
`critic/rewards/mean`	Mean predicted rewards. Key indicator of training progress. Should generally increase.
`response_length/mean`	Average response length in tokens. Bounded by max_response_length. Interpret alongside rewards.
`response_length/clip_ratio`	Response truncation ratio (responses hitting max length). **NOT related to PPO clip_ratio.** High = responses being cut off.
`timing_s/step`	Time per step. Sudden increases may indicate memory issues or inefficient batch sizes.
`perf/max_memory_reserved_gb`	Max GPU memory reserved. Monitors OOM risk. Helps optimize batch sizes.

Figure 6: Human-written metric descriptions injected into agent prompts to ground LLM reasoning about training dynamics.

Hyperparameter Reference Guide (injected into proposer prompt; LLM not restricted to this list)

Learning Rates & Optimization	
`weight_decay`	L2 regularization. Increase if large train/val gap; decrease if underfitting.
`grad_clip`	Max gradient norm. Decrease if NaN losses or collapse; increase if gradients consistently small.
Batch Sizes	
`ppo_micro_batch_size_per_gpu`	Micro-batch for gradient accumulation. Critical: ppo_mini_batch_size must be divisible by this.
PPO/GRPO Clipping	
`clip_ratio_low`	PPO lower bound. Keep at default; increasing may collapse sampling space.
`clip_ratio_high`	PPO upper bound. Higher values enhance entropy and diversity.
KL Divergence & Regularization	
`kl_loss_coef`	KL loss weight constraining policy changes. Only increase if KL spikes coincide with reward collapse.
`entropy_coeff`	Entropy bonus weight. **Critical: must remain 0 for GRPO.**
`norm_adv_by_std_in_grpo`	Normalize advantages by std. Generally keep True for stability.
Rollout & Sampling	
`rollout.n`	Samples per prompt. Higher improves advantage estimates, increases compute linearly.
`temperature`	Sampling temperature. Higher increases exploration and diversity.
Sequence & Memory Management	
`max_response_length`	Max response tokens. Increase if response_length/clip_ratio is high.
`max_num_seqs`	Max concurrent vLLM sequences. Decrease if OOM; increase for GPU utilization.
`tensor_model_parallel_size`	GPUs for model sharding. Use minimum that fits in memory.
Training Configuration	
`total_epochs`	Passes through data. Increase if validation still improving at final epoch.

Figure 7: Human-written hyperparameter descriptions injected into the proposer prompt, organized by functional category.

Proposer Agent Prompt Template

```
You are a hyperparameter optimization expert. Your goal is to maximize the validation
score by proposing hyperparameter changes for the next training run.

{previous_training_config}

{early_stop_notice}

### Training Step Metrics Summary
The training ran for {training_steps} steps:

{step_metrics_summary}

{metric_descriptions}

{hyperparameter_guide}

### Metric Interpretation
**PRIMARY:** Rewards (critic/rewards/mean) and validation scores measure overall
performance. Judge success by these metrics.
**DIAGNOSTIC:** actor/entropy, actor/kl_loss, actor/grad_norm, etc. Only relevant
when primary metrics degrade. Rising KL with stable rewards is acceptable.

### Your Task

Follow these steps **in order**. Do NOT suggest `total_epochs` until Step 4.

**Step 1 - Diagnosis:** Summarize the training health. What are the key trends in
primary metrics? Is the run healthy, plateauing, or collapsing? Note any inflection
points or anomalies.

**Step 2 - Hyperparameter suggestions:** Based on your diagnosis, propose specific
hyperparameter changes for the next run. Do NOT include `total_epochs` here
(computed in Step 4).
{suggestion_count_guidance}

**Step 3 - Checkpoint decision:**
{checkpoint_info}

**Step 4 - Epoch computation:** Now that you have decided all hyperparameters
(including `train_batch_size`) and the checkpoint strategy, compute `total_epochs`:
- If resuming: old_steps_per_epoch = total_training_steps / old_total_epochs,
  new_steps_per_epoch = old_steps_per_epoch * old_batch_size / new_batch_size,
  total_epochs = ceil((resume_step + ADDITIONAL_TRAINING_STEPS) / new_steps_per_epoch)
- If training from scratch: choose `total_epochs` based on target training steps
  and new batch size.

Show the math explicitly.
```

Figure 8: Proposer agent prompt template. Placeholders are filled with run-specific data at each search iteration.

Early Stopper Agent Prompt Template

```
You are an expert at analyzing RL for LLM post training using visual plots. Your task
is to decide if a run should continue or stop early.

### Objective
Your ONLY goal is to maximize the validation score. CONTINUE if the current run's
validation score trajectory has potential to exceed the best validation score seen so
far. STOP only when there is no realistic chance of beating it.

### Best Run Information
{best_run_summary}

### Current Run Progress (at checkpoint)
{current_run_summary}

### Visual Comparison
The plots show training metrics over time. Blue = current run, green dashed = best
run, both may start from an intermediate checkpoint.

Focus on the **validation score plot**. Ask: can the blue curve's peak eventually
exceed the green curve's peak?

{metric_descriptions}

### Decision Rules
**Default action is CONTINUE.** When uncertain, CONTINUE. Only STOP if ALL of these
are true:
1. Current step >= 10 (too early to judge before that)
2. The validation score trajectory has no realistic chance of exceeding the best
   validation score seen so far, considering the improvement rate, not just the
   current value. A run behind the best can still win if its trajectory is steeper;
   a run ahead can still lose if it is plateauing.

**Only the validation score determines STOP/CONTINUE.** All other metrics (rewards,
entropy, KL, gradient norms, clip_ratio, etc.) provide context but NEVER justify
stopping on their own.

**Response Format:**
REASON: [1-2 sentences on whether the validation score trajectory can beat the best
validation score seen so far]
DECISION: [CONTINUE or STOP]
```

Figure 9: Early stopper agent prompt template. Invoked every 900 seconds during training.

Table 18: Random search per-run results. GPU-hrs on 32×A100. Best Val = best validation score achieved. Test reported at best validation step. **Bold**: best per task.

Task	Run	GPU-hrs	Best Val	Best Step	Test
PaperSearchQA	00	470.6	0.370	234	0.360
	01	171.1	**0.392**	93	0.376
	02	198.5	0.370	36	0.366
	03	1740.6	0.384	84	0.358
	04	837.8	0.386	198	0.356
	05	1081.9	0.384	165	0.354
	06	510.8	0.384	198	0.364
	07	191.7	0.390	45	**0.384**
WildSci	00	602.3	0.604	147	0.565
	01	240.8	0.600	72	0.555
	02	577.7	0.612	72	0.559
	03	580.1	0.628	138	**0.580**
	04	1137.4	**0.630**	177	0.558
	05	295.6	0.610	132	0.544
	06	451.0	**0.630**	66	0.578
	07	806.7	0.602	27	0.540
SSMR-Bench	00	2193.9	0.708	186	0.682
	01	779.5	0.696	120	0.614
	02	575.1	0.754	213	0.696
	03	1536.0	—	—	—
	04	551.3	0.758	189	0.738
	05	279.8	**0.778**	57	**0.744**
	06	483.1	0.550	36	0.516
	07	431.6	0.688	57	0.660
ChemCoT	00	324.1	0.288	189	0.334
	01	1095.5	0.288	165	0.330
	02	356.9	0.270	30	0.297
	03	1015.2	0.304	255	0.316
	04	258.0	0.272	27	0.280
	05	504.4	0.282	228	0.324
	06	461.5	**0.320**	354	**0.394**
	07	527.1	0.290	174	0.313

Intended use consistency. All datasets are used for their intended purpose of evaluating language model capabilities on domain-specific reasoning tasks. VeRL and Ray are used for distributed RL training, consistent with their documented use cases.

Artifact documentation. We use 4 evaluation datasets (5,000 train / 500 val / 500 test each), Qwen3 models (0.6B–8B) with LoRA fine-tuning, a modified version of VeRL for GRPO training, and Ray for distributed orchestration on EKS clusters with A100 GPUs. All datasets are publicly available. We do not release trained model weights; we release discovered strategy configurations to enable reproduction. Upon acceptance we will additionally release the search framework code, all discovered strategy configurations, the task reward functions, and the full agent prompts (proposer and early stopper) to support reproducibility. Our new experiments on the public VeRL 0.7.1 release (Appendix E) re-confirm the main claims on a fully public stack, independent of the internal VeRL build used for the main results.

K Use of AI

We used AI-based tools to assist with grammar and writing clarity of the paper.

Table 19: Grid search per-run results. Grid varies LR $\in$ {1e-5, 3e-5, 5e-5, 1e-4} $\times$ LoRA rank $\in$ {64, 128}, while SSMR-Bench uses LR $\in$ {1e-5, 3e-5, 5e-5, 1e-4} $\times$ LoRA rank $\in$ {16, 32, 64, 128} to explore broader search space; all other HPs at default. **Bold**: best per task.

Task	Run	LR	Rank	GPU-hrs	Best Val	Test
PaperSearchQA	08	1e-5	64	372.6	0.398	0.390
	09	3e-5	64	383.5	0.384	0.390
	10	5e-5	64	387.8	0.394	0.388
	11	1e-4	64	397.8	0.396	**0.396**
	12	1e-5	128	424.4	0.392	0.384
	13	3e-5	128	1230.5	0.388	0.372
	14	5e-5	128	411.4	0.386	0.380
	15	1e-4	128	1299.3	**0.408**	0.372
WildSci	08	1e-5	64	711.2	0.616	0.551
	09	3e-5	64	2112.0	0.622	0.568
	10	5e-5	64	714.0	0.626	0.572
	11	1e-4	64	715.1	**0.650**	0.530
	12	1e-5	128	763.9	0.620	0.575
	13	3e-5	128	762.5	0.632	**0.580**
	14	5e-5	128	1545.3	0.626	0.558
	15	1e-4	128	770.5	0.632	0.576
ChemCoT	08	1e-5	64	684.5	0.296	0.327
	09	3e-5	64	703.2	0.308	0.350
	10	5e-5	64	725.5	0.304	0.351
	11	1e-4	64	1491.0	0.302	0.377
	12	1e-5	128	759.4	0.302	0.314
	13	3e-5	128	2038.7	0.318	**0.381**
	14	5e-5	128	766.4	**0.322**	0.350
	15	1e-4	128	2062.4	0.320	0.363

Table 20: Skill-based LLM agent per-iteration results. GPU-hrs reported per iteration. Budget-limited due to API cost ($635–1,146 per task). Best Val = best validation score at any step within the iteration.

Task	Iter	GPU-hrs	State	Best Val	Best Step	Test
PaperSearchQA	1	4.7	Failed	—	—	—
	2	3.8	Failed	—	—	—
	3	165.7	Cancelled	0.384	50	0.384
	4	137.1	Cancelled	0.392	80	0.366
	5	167.9	Completed	0.392	120	0.394
	6	8.6	Failed	0.374	200	0.386
	7	161.5	Completed	**0.396**	260	**0.402**
	8	6.0	Failed	—	—	—
	9	53.0	Cancelled	0.376	160	0.394
WildSci	1	136.8	Cancelled	0.591	20	0.561
	2	71.7	Cancelled	0.593	25	0.571
	3	110.8	Cancelled	0.619	45	0.538
	4	111.8	Cancelled	**0.621**	55	0.566
	5	17.1	Completed	0.597	75	0.570
	6	39.8	Cancelled	0.611	75	**0.603**
SSMR-Bench	1	328.8	Cancelled	0.828	90	0.820
	2	21.2	Completed	0.816	81	0.788
	3	48.1	Cancelled	**0.846**	85	0.800
	4	64.2	Completed	0.824	101	0.820
	5	65.4	Completed	0.814	105	0.796
	6	72.2	Cancelled	0.814	105	0.804
ChemCoT	1	399.7	Cancelled	0.281	125	0.376
	2	23.8	Failed	0.253	120	0.371
	3	55.4	Cancelled	0.271	125	0.334
	4	96.6	Cancelled	**0.299**	130	**0.380**
	5	46.8	Cancelled	0.291	140	0.380
	6	47.3	Cancelled	0.295	140	0.377
	7	39.2	Cancelled	0.259	125	0.356

Table 21: LLMZERO per-node results on SSMR-Bench (10 nodes, 64×A100). Val = aggregate validation score. Test = average of 4 subtask test scores at best validation step. ES = early-stopped.

Node	Wall-hrs	GPU-hrs	Status	Best Val	Best Step	Test (avg)
0	4.5	291	Completed	0.700	30	0.658
1	2.5	162	ES	0.672	33	0.658
2	2.5	162	ES	0.682	36	0.682
3	7.0	451	ES	0.732	66	0.706
4	13.2	846	Completed	0.830	153	0.822
5	**7.3**	**467**	**ES**	**0.870**	**180**	**0.822**
6	12.8	821	ES	0.764	99	0.738
7	5.8	371	ES	0.558	48	0.526
8	2.5	162	ES	0.858	195	0.838
9	6.7	428	Crashed	0.856	192	0.818
Total		**4,159**				

Table 22: LLMZERO per-node results on ChemCoT (16 nodes, 64×A100). Test = avg(und_avg, edit_avg, rxn_avg) at best validation step.

Node	Wall-hrs	GPU-hrs	Status	Best Val	Best Step	Test (avg)
0	7.3	469	Completed	0.292	36	0.330
1	4.6	294	Fix needed	0.312	72	0.359
2	2.6	164	ES	0.310	78	0.336
3	4.4	284	Completed	0.332	117	0.374
4	2.6	163	ES	0.326	120	0.368
5	2.8	180	ES	0.328	132	0.386
6	7.6	484	ES	0.264	36	0.313
7	5.6	356	ES	0.230	27	0.224
8	6.6	422	ES	0.246	30	0.264
9	7.2	460	Fix needed	0.266	18	0.302
10	13.9	889	ES	0.324	60	0.384
11	**15.5**	**992**	**Fix needed**	**0.356**	**180**	**0.406**
12	40.1	2,566	Debug	0.322	96	0.356
13	8.1	516	ES	0.322	78	0.380
14	2.6	164	ES	0.330	126	0.377
15	25.2	1,610	ES	0.330	120	0.374
Total		**10,013**				

Table 23: LLMZERO per-node results on PaperSearchQA (16 nodes, 32×A100). Test = single-metric test score at best validation step.

Node	Wall-hrs	GPU-hrs	Status	Best Val	Best Step	Test
0	19.1	611	Completed	0.388	114	0.390
1	15.7	501	Completed	0.408	123	0.410
2	18.8	601	Completed	0.408	141	0.422
3	4.0	129	ES	0.396	144	0.400
4	3.5	113	ES	0.390	123	0.400
5	**22.3**	**714**	**Completed**	**0.420**	**303**	**0.426**
6	40.0	1,281	Completed	0.390	246	0.378
7	5.5	177	ES	0.402	165	0.398
8	6.0	193	ES	0.414	306	0.424
9	10.0	321	ES	0.400	141	0.396
10	6.3	201	ES	0.402	162	0.398
11	40.0	1,281	Completed	0.380	300	0.372
12	4.0	129	ES	0.398	147	0.400
13	3.5	113	ES	0.396	162	0.402
14	4.0	129	ES	0.392	165	0.400
15	4.8	153	ES	0.404	171	0.406
Total		**6,646**				

Table 24: LLMZERO per-node results on WildSci (16 nodes, 32×A100). Test = average of 9 domain test scores at best validation step.

Node	Wall-hrs	GPU-hrs	Status	Best Val	Best Step	Test (avg)
0	7.3	234	Completed	0.608	36	0.548
1	10.3	329	ES	0.626	51	0.548
2	16.8	537	Completed	0.624	105	0.551
3	9.3	297	ES	0.618	54	0.565
4	14.6	466	ES	0.632	159	0.574
5	14.5	464	Completed	0.620	96	0.593
6	30.0	960	Completed	0.636	189	0.586
7	17.5	560	Completed	0.628	186	0.573
8	7.8	249	ES	0.636	210	0.589
9	7.0	225	ES	0.636	216	0.573
10	14.1	450	ES	0.630	216	0.569
11	40.0	1,281	Completed	0.622	120	0.560
12	4.0	129	ES	0.620	195	0.588
13	9.8	313	ES	0.622	153	0.563
14	13.8	442	ES	0.620	129	0.586
15	**13.6**	**436**	**Completed**	**0.640**	**174**	**0.585**
Total		**7,370**				

Algorithm 1 LLMZERO adaptive strategy discovery loop

Require: Dataset $\mathcal{D}$, base model M_0, budget B

Initialize root node n_0 with default configuration θ_0
Run initialization agents (data perception, task descriptor, tool selector)
for $t = 1$ to B **do**
  $n_{\text{parent}} \leftarrow$ SELECTNODE(tree) {UCT selection (Appendix F.2)}
  if n_{parent} failed **then**
    $(\theta_{\text{new}}, \text{fix}) \leftarrow$ ERRORANALYZER(n_{parent}) {Diagnose and propose fix}
  else
    $(\theta_{\text{new}}, k) \leftarrow$ PROPOSER(n_{parent}.metrics, n_{parent}.plots) {Multimodal analysis}
  end if
  $n_{\text{new}} \leftarrow$ CREATECHILD(n_{parent}, θ_{new}, checkpoint step k)
  Generate and submit training code via multi-agent pipeline (§3.6)
  while training in progress **do**
    Sample metrics and generate comparison plots at intervals
    if EARLYSTOPPER(current metrics, best strategy plots) = `STOP` **then**
      Terminate training early
    end if
  end while
  $s \leftarrow$ best validation score observed during run
  BACKPROPAGATE(n_{new}, s); PRUNETERMINAL(n_{new})
end for
return Strategy (scratch-to-leaf path) with highest validation score